

## ABSTRACT

Title of Dissertation:

DEVELOPMENT OF BIOMEMS DEVICE AND  
PACKAGE FOR A SPATIALLY  
PROGRAMMABLE BIOMOLECULE  
ASSEMBLY

Jung Jin Park, Doctor of Philosophy, 2006

Dissertation directed By:

Professor Gary W. Rubloff  
Department of Materials Science and Engineering  
and the Institute for Systems Research

We report facile *in situ* biomolecule assembly at readily addressable sites in microfluidic channels after complete fabrication and packaging of the microfluidic device. Aminopolysaccharide chitosan's pH responsive and chemically reactive properties allow electric signal-guided biomolecule assembly onto conductive inorganic surfaces from the aqueous environment, preserving the activity of the biomolecules. Photoimageable SU8 is used on a Pyrex bottom substrate to create microfluidic channels and a PDMS layer is sealed to the SU8 microchannel by compression of their respective substrates between additional top and bottom Plexiglas plates at the package level. Transparent and non-permanently packaged device allows consistently leak-free sealing, simple *in situ* and *ex situ* examination of the assembly procedures, fluidic input/outputs for transport of aqueous solutions, and electrical ports to guide the assembly onto the patterned gold

electrode sites within the channel. Facile post-fabrication *in-situ* biomolecule assembly of internal electrodes is demonstrated using electrodeposition of a chitosan film on a patterned gold electrode. Both *in situ* fluorescence and *ex situ* profilometer results confirm chitosan-mediated *in situ* biomolecule assembly, demonstrating a simple approach to direct the assembly of biological components into a completely fabricated device. We believe that this strategy holds significant potential as a simple and generic biomolecule assembly approach for future applications in complex biomolecular or biosensing analyses as well as in sophisticated microfluidic networks as anticipated for future lab-on-a chip.

**DEVELOPMENT OF BIOMEMS DEVICE AND PACKAGE FOR A SPATIALLY  
PROGRAMMABLE BIOMOLECULE ASSEMBLY**

by

Jung Jin Park

Dissertation submitted to the Faculty of the Graduate School of the  
University of Maryland, College Park, in partial fulfillment  
of the requirements for the degree of  
Doctor of Philosophy  
2006

Advisory Committee:

Professor Gary W. Rubloff, Chair  
Professor Reza Ghodssi  
Professor Gregory F. Payne  
Professor Robert M. Briber  
Professor Lourdes G. Salamanca-Riba

©Copyright by

Jung Jin Park

2006

## DEDICATION

To God and my family

## ACKNOWLEDGEMENTS

I am especially grateful to my advisor Dr. Gary W. Rubloff. He gave me the chance to work in an area I really like, provided me with great working environment and guided me throughout my study in his group.

I would like to acknowledge bioMEMS group members: Hyunmin Yi, Xiaolong Luo, Susan Beatty, Israel Perez, Sheng Li, Stephan Koev, Erin Dreyer, Li-Qun Wu, Rohan Femandes, Michael Powers, and Dr. Anand Gadre.

I also want to thank Dr. Mariano Anderle and his group in ITC-irst, Italy for their characterization work and delightful discussions.

I also want to thank my previous and current group members for their help in my work Laurent Henn-Lecordier, Erin Robertson, Wei Lei, Ernie Cleveland, Theresa Valentine, Yuhong Cai, Soon Cho, Jae-ouk Choo, Ramaswamy Sreenivasan, Rinku Parikh for their help in my work.

The author would like to thank Sheng Li for his generous help in using the clean room facility in MEMS Sensors and Actuators Lab (MSAL) at the University of Maryland in College Park.

This work was supported in part by the NSF under the MRSEC program and the IMI program and by the Laboratory for Physical Sciences.

## TABLE OF CONTENTS

<b>ABSTRACT</b> .....	<b>1</b>
<b>DEDICATION</b> .....	<b>ii</b>
<b>ACKNOWLEDGEMENTS</b> .....	<b>iii</b>
<b>TABLE OF CONTENTS</b> .....	<b>iv</b>
<b>LIST OF FIGURES</b> .....	<b>vi</b>
<b>LIST OF ABBREVIATION</b> .....	<b>viii</b>
<b>LIST OF ABBREVIATION</b> .....	<b>viii</b>
<b>Chapter 1 Introduction</b> .....	<b>1</b>
1-1 BioMEMS.....	1
1-2 Biomolecule assembly .....	3
1-3 Microfluidics .....	5
1-4 Research objectives, challenges and contributions.....	9
<b>Chapter 2 Chitosan electrodeposition</b> .....	<b>15</b>
2-1 Chitosan electrodeposition mechanism .....	15
2-2 Biomolecule assembly on the electrodeposited chitosan template.....	17
<b>Chapter 3 Novel Wafer Scale Microfluidic System Design and Fabrication .....</b>	<b>26</b>
3-1 Microfluidic device wafer design .....	26
3-2 Fabrication .....	27
3-2-1 Pyrex substrates for microfluidic device wafer.....	27
3-2-2 Gold electrode patterning and SU8 microchannel fabrication .....	28
3-3 Design and Fabrication of Microfluidic Package .....	29
3-4 Non-permanent compression sealing and leak test.....	31
<b>Chapter 4 <i>In situ</i> chitosan electrodeposition in completely packaged microfluidic devices</b> .....	<b>41</b>
4-1 Overview .....	41
4-2 Experimental condition.....	42
4-2-1 Electrodeposition of fluorescein labeled chitosan film .....	42
4-2-2 Fluorescent labeling of electrodeposited chitosan film.....	43
4-3 Results .....	44
4-3-1 Fluorescently labeled chitosan deposition in microfluidic channels.....	44
4-3-2 Fluorescent labeling of electrodeposited chitosan .....	45
<b>Chapter 5 Chitosan-mediated <i>in situ</i> biomolecular assembly in completely packaged microfluidic devices</b> .....	<b>54</b>

5-1 Overview .....	54
5-2 Experimental condition.....	55
5-1-1 GFP assembly on electrodeposited chitosan film .....	56
5-2-2 DNA assembly/hybridization in microfluidic system .....	56
5-3 Result.....	57
5-3-1 Post-fabrication <i>in situ</i> GFP assembly onto electrodeposited chitosan scaffold in the microfluidic channels.....	57
5-3-2 <i>In situ</i> probe DNA assembly onto electrodeposited chitosan scaffold and match target DNA hybridization in the microfluidic channels.....	59
<b>Chapter 6 Pfs-chitosan conjugate deposition and enzymatic reaction in completely packaged microfluidic devices .....</b>	<b>65</b>
6-1 Overview .....	65
6-2 Pfs-chitosan conjugate electrodeposition and enzymatic reaction in microfluidic system .....	66
6-3 Result: Enzyme reaction in microfluidic system .....	67
<b>Chapter 7 Conclusion .....</b>	<b>72</b>
<b>Chapter 8 Future work.....</b>	<b>78</b>
8-1 Multi steps of enzymatic reaction in microfluidic system.....	78
8-2 Integrated waveguide for real time optical detection of biocomponent in microfluidic system .....	79
<b>BIBLIOGRAPHY .....</b>	<b>82</b>

## LIST OF FIGURES

Figure 1-1 Examples of bioMEMS devices (a) Data knife smart scalpel (b) Scheme of a human implantation of the long term sensor system (c) Microneedle array d) DNA microarray (e) Integrated DNA analysis device .....	13
Figure 1-2 Schematic drawing of biomolecule assembly techniques (a) Preparation of SAMs (b) Micro contact printing (c) UV photo patterning (d) DPN (Dip-pen nanolithography).....	14
Figure 2-1 pH dependant protonation/deprotonation of chitosan molecule .....	19
Figure 2-2 Schematic view of chitosan deposition (a) No voltage is applied to Au electrode (b) Negative voltage is applied and pH gradient generated near the electrode surface (c) Negative voltage is applied for longer period of time and chitosan film gets thicker.....	20
Figure 2-3 (a) Electrodeposition of fluorescently labeled chitosan on patterned gold electrode (b) Fluorescence micrographs of fluorescently labeled chitosan deposited on electrodes with different line widths and shapes.....	21
Figure 2-4 (a) Chitosan thickness vs. deposition time (b) Chitosan thickness vs. current density (c) AFM image of chitosan film deposited with constant current (d) AFM image of chitosan film deposited with constant voltage (e) Chitosan hydrogel formation .....	22
Figure 2-5 XPS analysis on electrodeposited chitosan film surface .....	23
Figure 2-6 (a) Electrodeposited fluorescently labeled chitosan on patterned electrode (b) Chitosan-mediated protein assembly (c) Cell adhesion on chitosan film (d) Schematic drawing of virus assembly on chitosan via DNA cross linker.....	24
Figure 2-7 Schematic view of chitosan deposition in a microfluidic channel.....	25
Figure 3-1 (a) Design of microfluidic device wafer and 3-D view of test site X (b) Optical microscopy image of SU8 sidewall and microfluidic channel (c) Magnified image of patterned gold (1mm x 1mm) underneath SU8 microfluidic channel .....	33
Figure 3-2 Microfluidic device wafer fabrication process flow .....	34
Figure 3-3 Plexiglas package design.....	35
Figure 3-4 Schematic view of microfluidic device packaging process .....	36
Figure 3-5 (a) Exploded view of the packaging system (b) Schematic side view of microfluidic package .....	37
Figure 3-6 (a) Plexiglas microfluidic package for microfluidic device wafer (b) Side view of Plexiglas microfluidic package (c) Microfluidic system under a microscope.....	38
Figure 3-7 Schematic view of microfluidic compression sealing.....	39
Figure 3-8 (a) Magnified image of microfluidic system with blue dye solution inside the channel (b)-(c) Microscope image of fluid inside reservoir and microfluidic channel.....	40
Figure 4-1 (a) Experimental set up for biomolecule assembly in microfluidic system (b) Magnified image of microfluidic system under the microscope .....	48
Figure 4-2 Schematic process flow of electrodeposition of fluorescently labeled chitosan inside microchannel .....	49

Figure 4-3	Schematic process flow of fluorescent labeling of electrodeposited chitosan inside microchannels .....	50
Figure 4-4	(a) Schematic drawing of chitosan electrodeposition at the negatively biased electrode in the microfluidic channel (b-d) Fluorescence micrographs of the assembly site in microchannel (b) Before deposition, (c) After deposition, (d) After final water rinsing. Chitosan deposition was carried out at $2\text{A}/\text{m}^2$ for 240 sec. ....	51
Figure 4-5	(a) After chitosan deposition (b) NHS-fluorescein solution filled in the microfluidic channel (c) After labeling reaction (d) Negative control channel (no bias) .....	52
Figure 4-6	(a) Fluorescently labeled chitosan film showing the areas/sections for fluorescence profile analyses (b) Image J surface plot (c) Image J plot profile (d) Thickness by mechanical profilometry .....	53
Figure 5-1	Schematic process flow of GFP assembly on electrodeposited chitosan inside a microchannel.....	61
Figure 5-2	Schematic process flow of DNA hybridization on electrodeposited chitosan inside a microchannel .....	62
Figure 5-3	(a) Fluorescence image of the assembly site after chitosan deposition (b) After glutaraldehyde reaction (c) After GFP reaction (d) Negative control (no bias) (e) GFP conjugated chitosan film (f) Image J fluorescence surface plot .....	63
Figure 5-4	(a) Bright field image of assembly site (b) Fluorescence image of the assembly site after chitosan deposition (c) After glutaraldehyde reaction (d) After probe DNA reaction (e) Negative control (mismatch target DNA reaction) (f) After match target DNA hybridization.....	64
Figure 6-1	Schematic design of multiple enzymatic reaction in microfluidic channel for biomolecular factory application .....	69
Figure 6-2	Schematic drawing of enzymatic conversion of SAH precursor to SRH and adenine by assembled Pfs-chitosan inside the microchannel (a) Pfs-chitosan conjugate introduction into microchannel (b) Electrodeposition of Pfs-chitosan (c) Enzymatic conversion of SAH precursor to SRH and adenine (d) HPLC analysis on the collected SRH and Adenine samples .....	70
Figure 6-3	(a) HPLC analysis result of sample collected from microfluidic system; (left) Electrode was charged for chitosan deposition and SAH precursor introduced over electrodeposited chitosan film (right) Negative control experiment (electrode was not charged for chitosan deposition) (b) Mechanical profilometry on the electrodeposited Pfs-chitosan film inside the microchannel.....	71
Figure 8-1	(a) Schematic design of multiple enzymatic reaction in microfluidic channel for biomolecular factory application (b) Microfluidic system design for biomolecular factory .....	80
Figure 8-2	(a) Fluorescent micrograph with a green fluorescein dye chitosan conjugate indicating successful sidewall deposition (b) 3-D image of fiber alignment structure .....	81

## LIST OF ABBREVIATION

<b>µm</b>	micrometer
<b>µM</b>	micromolarity
<b>µTAS</b>	micro total analysis systems
<b>A</b>	ampere
<b>AI-2</b>	autoinducer 2
<b>AFM</b>	atomic force microscope
<b>ALD</b>	atomic layer deposition
<b>AMU</b>	atomic mass unit
<b>BSA</b>	bovine serum albumin
<b>cm</b>	centimeter
<b>CMOS</b>	complementary metal-oxide semiconductor
<b>CMP</b>	chemical mechanical polishing
<b>CO<sub>2</sub></b>	carbon dioxide
<b>COPs</b>	cyclo-olefin polymers
<b>CTE</b>	coefficient of thermal expansion
<b>D</b>	dimension
<b>DI water</b>	deionized water
<b>DNA</b>	deoxyribonucleic acid
<b>DPN</b>	dip-pen nanolithography
<b>GFP</b>	green fluorescent protein
<b>HCl</b>	hydrochloric acid
<b>HPLC</b>	high performance liquid chromatography
<b>Hz</b>	hertz
<b>ID</b>	inside diameter
<b>ITO</b>	indium tin oxide
<b>LuxS</b>	S-ribosylhomocysteinate
<b>m</b>	meter
<b>MEMS</b>	microelectromechanical systems
<b>ml</b>	milliliter
<b>min</b>	minute
<b>mJ</b>	millijoule
<b>mm</b>	millimeter
<b>N<sub>2</sub></b>	nitrogen gas
<b>NaBH<sub>4</sub></b>	sodium borohydride
<b>NaOH</b>	sodium hydroxide
<b>NHS</b>	Carboxyfluorescein succinimidyl ester
<b>nm</b>	nanometer
<b>OH</b>	hydroxy
<b>PBS</b>	phosphate buffered saline
<b>PCR</b>	polymerase chain reaction
<b>PDMS</b>	polydimethylsiloxane
<b>Pfs</b>	S-adenosylhomocysteine nucleosidase
<b>PGMEA</b>	propylene glycol monomethylether acetate
<b>pl</b>	picoliter

<b>PMMA</b>	polymethyl methacrylate
<b>PPy</b>	polypyrrole
<b>RNA</b>	ribonucleic acid
<b>rpm</b>	revolutions per minute
<b>SAH</b>	S-adenosylhomocysteine
<b>SAM</b>	self assembled monolayers
<b>sec</b>	second
<b>SRH</b>	S-ribosylhomocystein
<b>TMV</b>	tobacco mosaic virus
<b>Tris</b>	trishydroxymethylaminomethane
<b>UV</b>	ultraviolet
<b>V</b>	volt
<b>XPS</b>	x-ray photoelectron spectroscopy

# **Chapter 1 Introduction**

## **1-1 BioMEMS**

Microfabrication technologies, such as photolithography, etching, thin film deposition and packaging, have evolved from semiconductor manufacturing processes commonly used in the fabrication of microprocessors and memory devices. These processes are now routinely used in the fabrication of MEMS (Micro Electro Mechanical System) devices.<sup>1,2</sup> Bulk and surface micromachining technique enables the fabrication of 2-D or 3-D structures made of inorganic or plastic materials. These structures can be static or dynamic and have been incorporated into a numbers of microscale devices such as sensors and actuators already used in everyday life.<sup>2-5</sup>

Recently the collaboration of biotechnology/biomedical engineering and MEMS, bioMEMS (Bio-Micro Electro Mechanical System) has significantly gained attention due to its broad applications and advantages in the realm of MEMS devices. Microdevices such as surgical micro sensors, diagnostic systems and therapeutic systems have been developed and are continually being researched.<sup>6</sup> Examples of bioMEMS devices in the areas are shown in Figure 1-1. Surgical micro system enables surgery on small blood vessels even smaller and provides micro invasive surgery which minimizes the size of an incision and reduces the recovery period.<sup>6,7</sup> Drug delivery systems employing a fluid dispensing mechanisms or micropumps can be implanted in the body. A sensor is integrated into the device where a feedback system loops the sensor and the drug dispensing actuator to deliver an adequate amount of drug to the body and frees the patient from external devices. A good example of an implantable drug delivery system is

an integrated glucose sensor and an insulin micro-dispenser for diabetic patients.<sup>8</sup> A transdermal micro-needle array is also developed to use an alternative route to deliver drugs through the skin instead of oral drug delivery. Its advantages include the absence of degradation in the gastrointestinal tract, first-pass effects in the liver, and the elimination of pain. Diagnostic micro systems based on miniaturization technologies are critical to rapid and inexpensive diagnoses of diseases. Biomolecular recognition sensors have been developed for rapid chemical analysis in a high throughput manner for laboratory use or disease detection. Products are usually disposable and cost effective due to the benefit of mass production of micro devices. A DNA (deoxyribonucleic acid) microarray has recently been developed and commercialized. The device allows a DNA hybridization analysis in a highly parallel and high throughput manner for genomic research applications which deal with a large number of base pair of DNA.<sup>9,10</sup> Typically different probe DNA or oligomer chains are immobilized on the array of micron scaled spots on the substrate with various immobilization techniques. Target free DNA or RNA (ribonucleic acid) chains which are usually fluorescently labeled are transported and hybridized to the microarray, followed by a microscopic scanning process revealing the different intensity of the label related to the degree of hybridization. A microfluidic based DNA analysis chip was also developed. An analyte sample is transported through a microchannel and undergoes filtration, PCR (Polymerase Chain Reaction), electrophoresis and detection processes in one chip, allowing faster DNA analysis process time which is usually a longer process when it is performed in laboratory.<sup>11</sup> Other biosensors have also been developed for biomolecule recognitions on relevant molecules such as glucose, lactic acid and ascorbic acid, as well as, the detection of environmental

agents.<sup>12, 13</sup> The sensing element is integrated with an electrochemical, optical or piezoelectric transducers. Other diagnostic micro systems employing different approaches are micro cantilevers and miniature mass spectrometers, demonstrating high sensitivity and resolving power on chemical species detection and analysis.<sup>14, 15</sup> Improvement of the design, microfabrication technology and development of novel micro devices enable the integration of devices in diagnostic micro system into one system. Trend indicates that pre-analysis steps such as filtration and amplification are integrated into analysis system or biosensors to achieve ‘micro total analysis system s ( $\mu$ TAS)’ or ‘lab on a chip’. This technology will not only revolutionize analytical chemistry/molecular biology research but will also leads to rapid disease diagnostic systems available for the individual home.<sup>16-18</sup>

In our research, we propose a new approach to develop a microfluidic based diagnostic micro system which includes a device and package level with a novel biomolecular assembly technique developed by our research collaborators at University of Maryland.

## **1-2 Biomolecule assembly**

One of the most critical issues in bioMEMS research is biomolecule assembly on a substrate of bioMEMS device. Currently several assembly techniques have been developed and some of them are shown in Figure 1-2.

An ink jet printing technique was used to deliver a small drop of chemical reagent which is confined to a small area on the substrate of the high density micro array.<sup>19</sup> The challenge is to deliver a small amount of chemical reagent to the appropriate spot and the

micro ink jet pump is fabricated to meet the requirement. A silicon wafer is etched to create a shallow channel and a cavity. A thin glass membrane is the anodically bonded to silicon to seal the cavity. A piezoelectric element is glued to the thin glass membrane and its pumping actuation could deliver 100 pl of a droplet on rates of several hundred Hz.

The use of SAM (self assembled monolayers) is a popular method to assemble biological components on solid substrates.[Figure 1-2 (a)]<sup>20</sup> Strong adsorption of sulfur-containing molecules such as disulfides (R-S-S-R), sulfides (R-S-R) and thiols (R-SH) on a gold surface forms highly ordered monolayers. Thiol-derivatized, single-stranded DNA (HS-ssDNA) can be attached to a gold surface via a sulfur-gold linkage.<sup>21</sup> Silane on metal oxides is also widely used as a SAM interface layer between biomolecules and a substrate.<sup>22</sup>

Microcontact printing developed by using stamp micro structures fabricated soft lithography from Whiteside's group.[Figure 1-2 (b)]<sup>23, 24</sup> A stamp made of an elastomeric material such as poly(dimethylsiloxane) (PDMS) can be topographically structured by casting the prepolymer against a 3-D master. The stamp is inked with the molecules of interest, blown dry under a stream of nitrogen, and then printed onto the substrate surface. This technique achieves a faster array fabrication and resolves the drying issue of ink jet printing methods which cause inhomogeneities at the rim around a spot.

UV photopatterning is similar to the process of photolithography employed in the production of Si-based microelectronics. [Figure 1-2 (c)] It has also been demonstrated that SAMs can be patterned in the plane of the surface photochemically by using photoactive pendant groups with micron scale resolution.<sup>25</sup> This method is compatible with optical imaging of a pattern and, consequently, does not require physical contact

with the SAMs. SAMs were formed on Au and Ag substrate and UV radiation was provided on the SAMs, degrading only the photoactive group from SAMs. The removed area is often chemically functionalized or selectively etched away. A schematic process is shown in Figure 1-2 (c).

DPN (Dip-pen nanolithography) is a technique that writes nanosized patterns using an AFM (Atomic Force Microscope) tip as a “nib” dipped in a solution of molecules (ink) on a solid substrate such as Au as “paper”. [Figure 1-2 (d)]<sup>26</sup> Molecules are delivered from the AFM tip to a solid substrate of interest via capillary transport to directly write patterns with submicrometer dimensions, making DPN a potentially useful tool for creating and functionalizing nanoscale devices like DNA/protein nano arrays.<sup>27</sup> DPN is a serial technique and has advantage over a parallel technique such as micro contact printing when different types of molecules need to be placed selectively.

While these methods are being rapidly developed and widely adapted, there are environmental factors that affect performances such as presence of interferents, denaturing agents, hydrophobic surface, and analyte concentration etc. These methods also employ pre-fabrication biomolecule assembly in incompletely packaged device so biological activity may be in risk during device manufacturing or storage period.

### **1-3 Microfluidics**

Microfluidics deals with the behavior, precise control and manipulation of microliter and nanoliter volumes of fluids and is a multidisciplinary field with practical applications such as lab on a chip technology, biosensors, biochemical analysis/synthesis, and drug discovery. Microfluidics is popularly used in the bioMEMS areas: capillary

electrophoresis, immunoassays, enzyme reaction kinetics, flow cytometry, PCR amplification, DNA analysis, cell manipulation, and cell separation.<sup>28-35</sup> The use of microfluidic devices to conduct biomedical research and create clinically useful technologies has a number of significant advantages. (1) Microfluidic devices require smaller reagent volumes which could be rare and expensive because the volume of fluids within these channels is very small. (2) They provide shorter reaction times compared to macroscale experiment. (3) Parallel operation is possible and it leads to rapid and high throughput of sample analysis. (4) The devices can also be disposable since the fabrication technology is relatively inexpensive and devices can be manufactured by mass production. (5) Microfluidic technologies similar to microelectronics enable the fabrication of highly integrated devices for performing multiplex functions on a miniaturized single chip, allowing portable systems to be available to the individuals in any places.

Various fabrication technologies that have been developed include micro machining, soft lithography, photolithography, embossing, and injection molding. Micro machining is widely used for silicon and glass based microfluidic device fabrication. Deposition, patterning, and etching processes are involved to fabricate microfluidic systems. This is suited to applications that require strong solvents and high temperature process. However, these processes are costly, labor intensive and require equipment and facilities. Soft lithography is one of the most popular fabrication techniques due to its fast process, inexpensive, and less specialized method. Whitesides and others have revolutionized the way soft lithography is used in microfluidics. This is a technique of molding a soft material, PDMS (Polymethylsiloxane), from a lithographic master. Hot embossing

technique is a technique of transferring a pattern from a micro machined master. A plastic material is deformed and become imprinted from a master with heat and high pressure. PMMA (Polymethyl methacrylate) and COPs (Cyclo-Olefin Polymers) are the most commonly used plastic materials with the hot embossing technique. Injection molding is a very promising technique, where molten plastic is injected into a cavity that contains the master. It is low cost and fast fabrication but its limitation in the resolution and material choice.

Microfluidic sealing is critical and various permanent sealing have been proposed. A variety of fluidic sealing technologies have been explored in the past, including fusion bonding, anodic bonding, and bonding with UV curable adhesives.<sup>36-40</sup> Fusion bonding is a direct bonding between silicon based materials (Si-Si, Si-SiO<sub>2</sub>, SiO<sub>2</sub>-SiO<sub>2</sub>) and requires high temperature processes. Surface roughness should be in the range of angstroms. First surfaces are hydrated to form hydrophilic O-H bonds and the surfaces initially stick together due to Van der Waal's bonding. Pressure is then applied and the materials are heated to the temperature range of 800 – 1100 °C in N<sub>2</sub>. Bond strength should be around 20 Mpa. Anodic bonding is often used for silicon – insulator bonding (e.g. SiO<sub>2</sub>, Si<sub>3</sub>N<sub>4</sub>). Insulators must contain mobile ions such as Na<sup>+</sup> ions. Silicon and an insulator are placed in contact and are heated around 300 – 450 °C, allowing ions to become mobile.<sup>39</sup> Subsequently a negative voltage is applied at the center of the glass wafer to attract mobile positive ions from the insulator to the electrode, leaving a negative charge at the glass/Si interface. Covalent bonds form the silicon and the insulator. Anodic bonding is a relatively lower temperature process than fusion bonding and surface roughness is in the nm range. It is also more robust than fusion bonding, but this process cannot be used

for CMOS (Complementary Metal-Oxide Semiconductor) chip since alkali metal ions are introduced during the process. Sealing of polymer microchannels is generally much simpler than with silicon or glass channels and can often be accomplished using low temperature thermal annealing. A lower glass transition temperature can be used to ensure that there are no deformations of the microchannel during the sealing process. To form a permanent seal with PDMS, plasma oxidation of the PDMS surfaces is performed to bond the material to itself or to other substrates including glass, silicon, silicon oxide, quartz, silicon nitride, polyethylene, polystyrene, and glassy carbon.<sup>38, 41</sup> However, each of these options entails some drawbacks. Elevated temperatures associated with thermal bonding can approach the softening temperature of the materials, leading to distortion of the microchannel structures; furthermore, biomolecules predeposited on the substrate may be unstable at the process temperature.<sup>38, 42</sup> Anodic or fusion bonding between silicone and glass materials can also require excursions of pressure, temperature, or voltage for an extended period of time, stressing the materials and structures of the bioMEMS. High voltages (~ 1 kV for a 400  $\mu\text{m}$  thick glass wafer) are required for anodic bonding and polishing or CMP (Chemical Mechanical Polishing) may be needed for surface planarization prior to bonding. The CTE (Coefficient of Thermal Expansion) match may be critical to minimize stresses in bonded wafers. Wafers should be brought together in a controlled manner to prevent trapped air pockets at either the flat/edge or center. Contamination-free surfaces should also be achieved by using a wet chemical cleaning can be done before bonding to prepare the surfaces. UV-curable adhesives are another common bonding method used for bonding dissimilar materials, however, the ultraviolet light employed may damage biomolecules already present in the bioMEMS.<sup>42</sup>

Each of these existing methods requires special steps and labor to complete the bonding, which if successful produces a permanent bond. It would be advantageous to have a simpler, robust design and fabrication approach that will avoid elevated process conditions, allows the reuse of components, and enables the microchannel network to be opened after use for post-operation, *ex-situ* analysis.

#### **1-4 Research objectives, challenges and contributions**

Microfluidic devices have recently gained significant attention due to their broad applications for biosensors<sup>43-46</sup>, biomedical synthesis/analysis applications<sup>41, 47-49</sup>, and metabolic engineering.<sup>50</sup> Recent advances in fabrication techniques significantly scaled down the dimensions allowing smaller sample sizes and high throughput screening capabilities for various analytical procedures such as capillary electrophoresis, PCR (Polymerase Chain Reaction) and drug screening.<sup>9, 43, 51, 52</sup> Despite such advances, assembling biological components in the microfluidic devices in their active forms with spatial selectivity still remains challenging.

Conventional methods to add biological components to devices include optical methods such as photolithography, mechanical methods such as ink jet printing, soft lithography and microcontact printing, involving chemical reactions at various stages.<sup>19, 23, 24, 53, 54</sup> While these methods are being rapidly developed and widely adapted, each method encounters limitations such as arduous chemical procedures, requirements for complicated robotic facilities, dry environment and lack of flexibility that may destroy activities of the biomolecules being assembled. It is thus highly desirable that the biomolecule assembly step to be performed *in situ* from the aqueous environment after complete fabrication and packaging of the device. We have been exploiting biopolymer

chitosan as the biomolecule assembly scaffold to achieve such goal.<sup>55</sup> Chitosan is an aminopolysaccharide with unique properties that can be harnessed to assemble biological molecules onto conductive surfaces. Each glucosamine monomer unit of chitosan has a primary amine group with a low pKa value ( $\approx 6.3$ ), which is protonated and positively charged at low pH, making chitosan soluble in aqueous solution. At neutral to high pH, this amine group becomes deprotonated and uncharged, thus making chitosan insoluble biopolymeric hydrogel networks. This pH-responsive property allows assembly of chitosan from aqueous solution onto a negatively biased electrode surface due to the high local pH near the electrode in a highly spatially selective manner.<sup>56, 57</sup> Further, this primary amine group is nucleophilic at neutral state thus allowing various amine group reactive chemistries to be used for covalent conjugation of biomolecules onto chitosan<sup>55, 58, 59</sup>. Combination of these two unique properties, namely pH-responsiveness and chemical reactivity, holds significant potential for post-fabrication biomolecule assembly in the microfluidic devices since the assembly of the chitosan scaffold occurs in response to electrical signal from the device to the aqueous solution, and the subsequent procedures for biomolecule conjugation are also carried out in closed aqueous environment avoiding drying, damaging or contamination.

In this research, we report the development of a microfluidic system to achieve post-fabrication biomolecule assembly in the microfluidic environment. Our microfluidic device design employs microfabricated SU8 on a Pyrex wafer as the knife-edge that defines the microfluidic channel structure, and patterned gold electrodes at the bottom of each microchannel as the readily addressable biomolecule assembly sites. Non-permanent and leak-tight sealing of the microfluidic channels at the device level is then

achieved by sealing the wafer with a PDMS-spun top sealing Plexiglas plate and then packaging with pressure-adjustable compression bolts. Finally, fluidic and electric input/output ports are connected to microchannels for micropump-driven transport and electric signal-guided assembly of biomolecules from the aqueous environment.

Taking advantage of this microfluidic system we then demonstrate post-fabrication, *in situ* biomolecule assembly using the electrodeposition of chitosan at readily addressable assembly sites within the microfluidic channels. In this work, we first use fluorescently labeled chitosan to directly demonstrate biomolecule assembly at specific electrodes inside a microfluidic channel within the completely packaged microfluidic device, indicating the potential of this platform for biomolecular reaction processes. We then assemble fluorescent marker molecules, fluorescein and green fluorescent protein (GFP), onto electrodeposited chitosan scaffold, illustrating electric signal-guided *in situ* biomolecule assembly at readily addressable sites in the microfluidic channels. These results demonstrate the first signal-guided chitosan-mediated biomolecule assembly in the microfluidic environment after complete packaging of the microfluidic device. We then further examine the biopolymeric scaffold by *ex situ* profilometer measurements, illustrating the advantage of our non permanent sealing/packaging strategy. As a next set of experiment, we deposited unlabeled chitosan film inside the microchannel and probe DNA was assembled onto the deposited chitosan film via glutaraldehyde crosslinking agent. Then target DNA was introduced into the microchannel and hybridized with the probe DNA assembled on the chitosan film, demonstrating signal-guided nucleic acid assembly on a specific site inside the microchannel. Finally we electrodeposited Pfs (S-adenosylhomocysteine nucleosidase) enzyme–chitosan conjugate inside the microchannel

and introduced reactant over the enzyme. Then SAH (S-adenosylhomocysteine) precursor will be introduced and enzymatically converted to SRH (S-ribosylhomocysteine) by Pfs on the chitosan surface. We then further analyzed converted samples with HPLC (High Performance Liquid Chromatography) to get conversion rate. We believe that this post-fabrication, *in situ* biomolecule assembly strategy would be readily applicable to future bioMEMS device designs that require simple approaches to multi-species biofunctionalization in two or three dimensional networks.<sup>60-62</sup> Especially, this work represents our ongoing efforts to harness microfabricated devices to actively engage biomolecular reactions, in this case by guiding spatially selective *in situ* biomolecule assembly through electric signals.

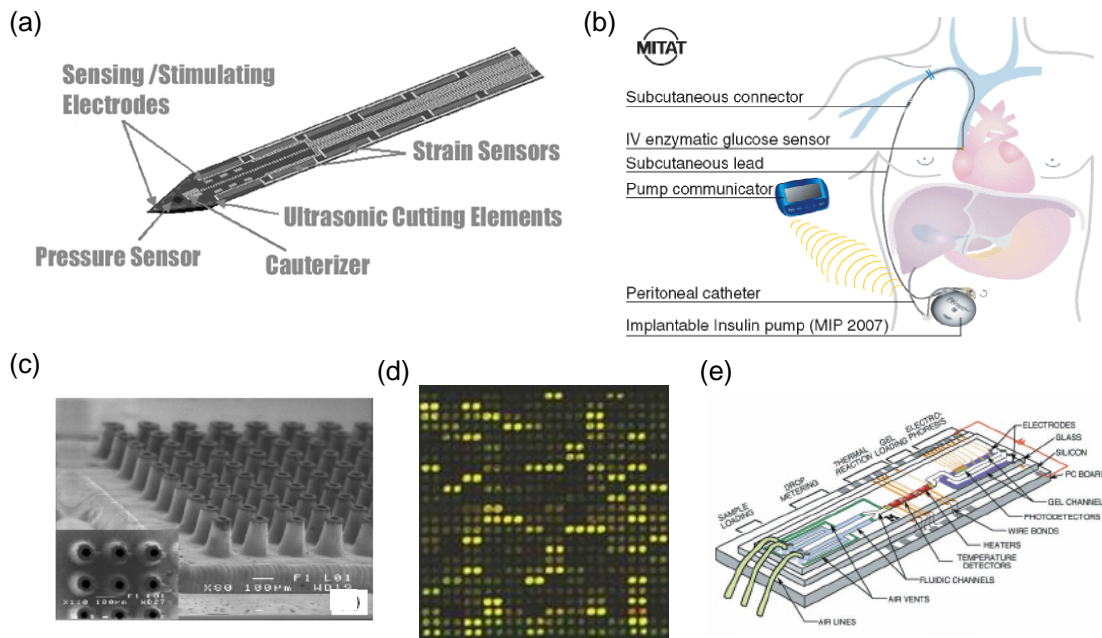


Figure 1-1 Examples of bioMEMS devices (a) Data knife smart scalpel (b) Scheme of a human implantation of the long term sensor system (c) Microneedle array d) DNA microarray (e) Integrated DNA analysis device

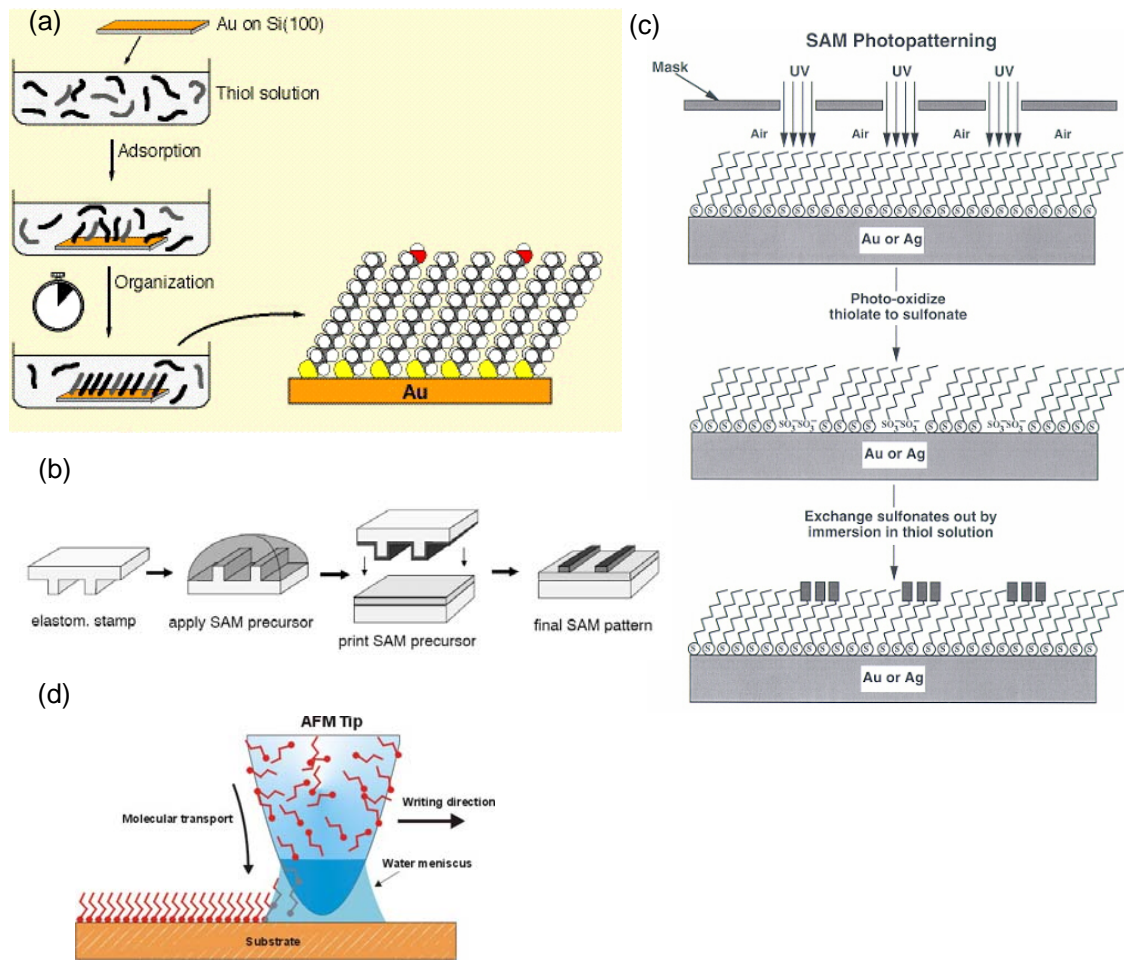


Figure 1-2 Schematic drawing of biomolecule assembly techniques (a) Preparation of SAMs (b) Micro contact printing (c) UV photo patterning (d) DPN (Dip-pen nanolithography)

## **Chapter 2 Chitosan electrodeposition**

### **2-1 Chitosan electrodeposition mechanism**

Chitosan is a linear polysaccharide composed of randomly distributed  $\beta$ -(1-4)-linked D-glucosamine (deacetylated unit) and N-acetyl-D-glucosamine (acetylated unit) and it is obtained by deacetylation of chitin. Chitin is the second most abundant polysaccharide in nature and is found in crustaceans, insects, and fungi.<sup>56</sup> Chitosan's primary amino group in each glucosamine monomer unit has pH responsive property. As shown in Figure 2-1, the amino group in chitosan has a pKa value of ~6.3, thus, chitosan is positively charged and soluble in acidic to neutral solution and is deprotonated and insoluble in high pH condition (> 6.3). This pH-responsive property allows spatially selective assembly of chitosan onto a negatively charged electrode surface. Chitosan is prepared in solution to be assembled on an inorganic surface. First chitosan flakes are put in DI water and dissolved in stirring condition while pH condition is maintained at 2~3 by adding HCl solution. After dissolving the flakes, the solution undergoes filtration step and NaOH is added to the solution to increase pH level near 5 which is known as an optimized chitosan deposition condition.<sup>63</sup>

To achieve chitosan assembly onto an electrode surface in spatially selective manner, a gold electrode is photolithographically patterned. Gold is chosen since it is chemically inert and easily patternable using typical photolithography technique.<sup>64</sup> For chitosan assembly, two gold electrodes, working and counter electrodes, are immersed in chitosan solution and they are connected to the power supply with alligator clips and the schematic view of chitosan deposition mechanism is shown in Figure 2-2. After two electrodes are

immersed in the low pH chitosan solution, the cathode is negatively biased and proton consumption occurs at the cathode and instantly water molecules dissociate to compensate proton and OH accumulates near the surface of cathode. Therefore a pH gradient is generated near the surface of cathode, depending on the relative rates of hydroxyl ion generation. Simultaneously chitosan molecule which is electrostatically transported to the cathode and in the high pH region near the cathode, are deprotonated and immobilized.<sup>56</sup> The electrodeposition technique allows highly spatially selective assembly of chitosan on the patterned negative electrode and 20  $\mu\text{m}$  resolution of electrodeposition of chitosan on a patterned surface has been reported [Figure 2-3]<sup>57</sup> and we recently achieved chitosan deposition on 2  $\mu\text{m}$  gold line. Importantly electrodeposition chitosan can be performed on various shape of patterned electrode [Figure 2-3 (b)] and possibly 2-D or 3-D structures of complex microscale network since deposition process occurs in aqueous condition and it is not inhibited by geometric factor. Another advantage of this material is that we can control the thickness, morphology and structure with different conditions. We can control it with deposition process conditions such as deposition time and current density.<sup>65</sup> Figure 2-4 shows mechanical profilometry on the deposited chitosan films, indicating chitosan film thickness is proportional to the current density and deposition time. Chitosan films were deposited with constant current condition ( $2 \text{ A/m}^2$ ) and profilometry result shows that the thickness of chitosan film increases with deposition time. About 250 nm/min deposition rate was obtained. Next, chitosan films were deposited with different current density and constant deposition time (180 sec). Figure 2-4 (b) shows profilometry result, demonstrating that chitosan thickness increases with current density. Figure 2-4 (c) - (d) shows AFM analyses

performed on electrodeposited chitosan surface. Result shows that the morphology of the chitosan film deposited with constant voltage is flatter than the one deposited with constant current condition, resulting increasing surface roughness moving from constant voltage to constant current with different deposition time. Finally, structure of chitosan deposited can be varied with deposition conditions. As shown in Figure 2-4 (e), a chitosan hydrogel can be formed on the gold electrode with higher current density 50 A/m<sup>2</sup> for 20 min, indicating that the structure of chitosan electrodeposited could be controlled easily by changing deposition condition.<sup>63</sup> This result indicates that 3-D chitosan structure can be formed and can be used for biological research which requires biofriendly environment. As a different approach, biolithography technique has also been developed and thermoresist gelatin can be patterned on the chitosan film surface, demonstrating simple fabrication of environmental friendly biomaterial structure.<sup>66</sup>

## 2-2 Biomolecule assembly on the electrodeposited chitosan template

Electrodeposited chitosan film has abundant amine group and XPS analysis in the Figure 2-5 shows oxygen, carbon and especially nitrogen line obtained from the amine group of electrodeposited chitosan film, demonstrating that the surface chemistry does not depend on deposition method. It also revealed that incomplete deacetylation process during chitosan production leaves significant residual chitin precursor in chitosan film. The primary amine group is nucleophilic and enables covalent conjugation of biomolecules such as proteins and nucleic acids. Figure 2-6 shows that variety of biomolecules assembled onto electrodeposited chitosan in macro scale environment such as (a) fluorescently labeled chitosan on the patterned gold electrode (b) conjugation of

Texas Red labeled gelatin with chitosan and conjugation of GFP with chitosan (c) human osteoblast-like cells (MG-63) adhesion on chitosan surface via RGD (Arg-Gly-Asp) peptide cross linker and (d) DNA probe directed assembly of TMV (Tobacco Mosaic Virus ) on electrodeposited chitosan surface.<sup>57, 58, 67, 68</sup> These results demonstrate that chemical reactivity of chitosan enables facile biomolecule assembly on electrodeposited chitosan template, demonstrating signal guided biomolecule assembly on a specific assembly site. This chitosan-mediated biomolecule assembly technique developed can be used as a novel surface biomaterials platform for bioMEMS applications with spatial and temporal programmability of biomolecular reactions. Ultimately, we believe that the idea about spatially selective biomolecule assembly on the electrodeposited chitosan template can be performed in the microscale environment such as microfluidic system for simultaneous sample processing and detection as shown in Figure 2-7.

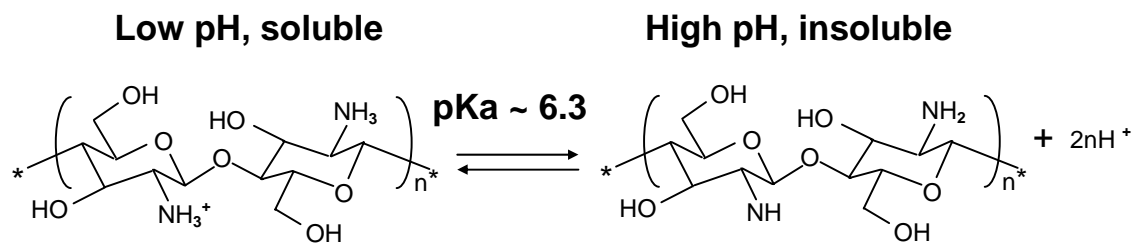


Figure 2-1 pH dependant protonation/deprotonation of chitosan molecule

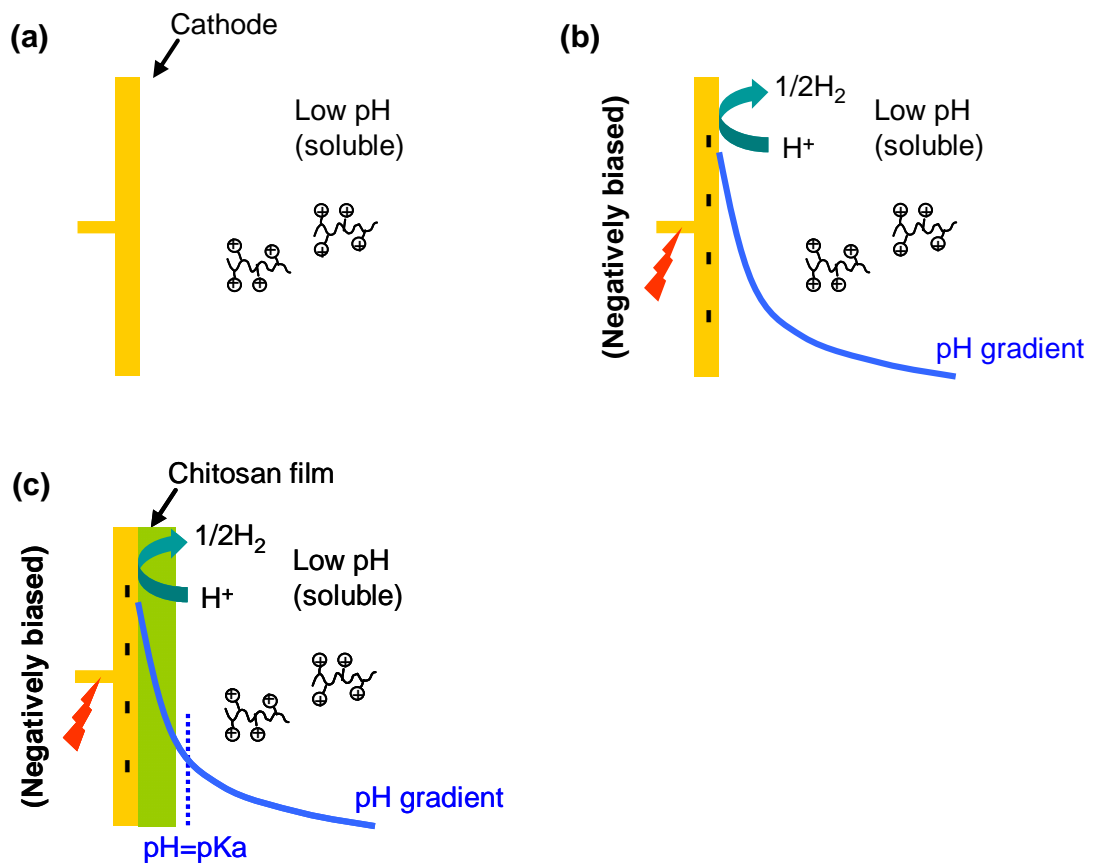


Figure 2-2 Schematic view of chitosan deposition (a) No voltage is applied to Au electrode (b) Negative voltage is applied and pH gradient generated near the electrode surface (c) Negative voltage is applied for longer period of time and chitosan film gets thicker

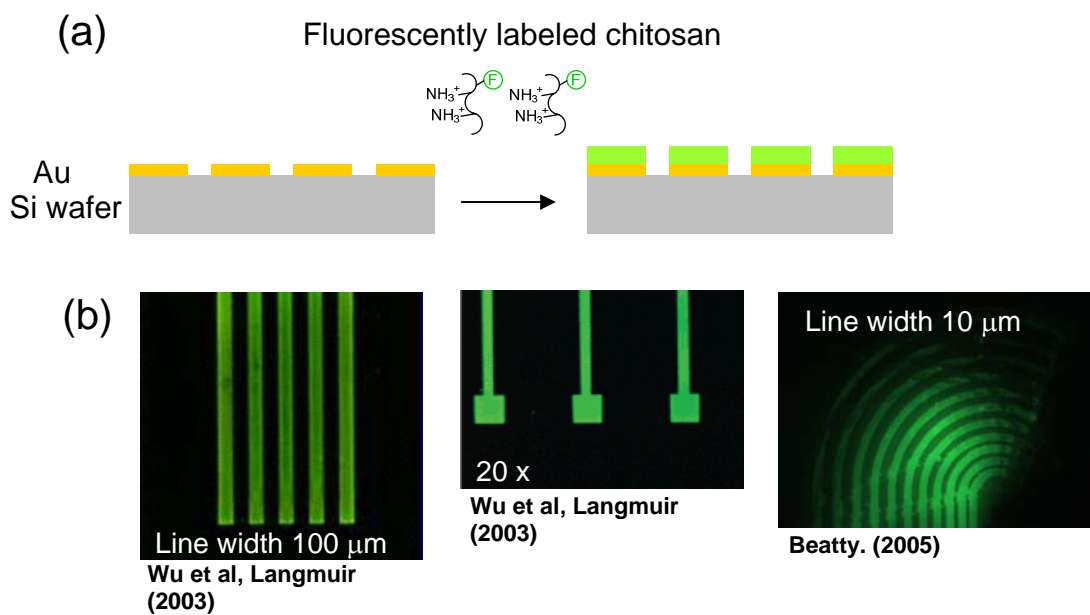


Figure 2-3 (a) Electrodeposition of fluorescently labeled chitosan on patterned gold electrode (b) Fluorescence micrographs of fluorescently labeled chitosan deposited on electrodes with different line widths and shapes.

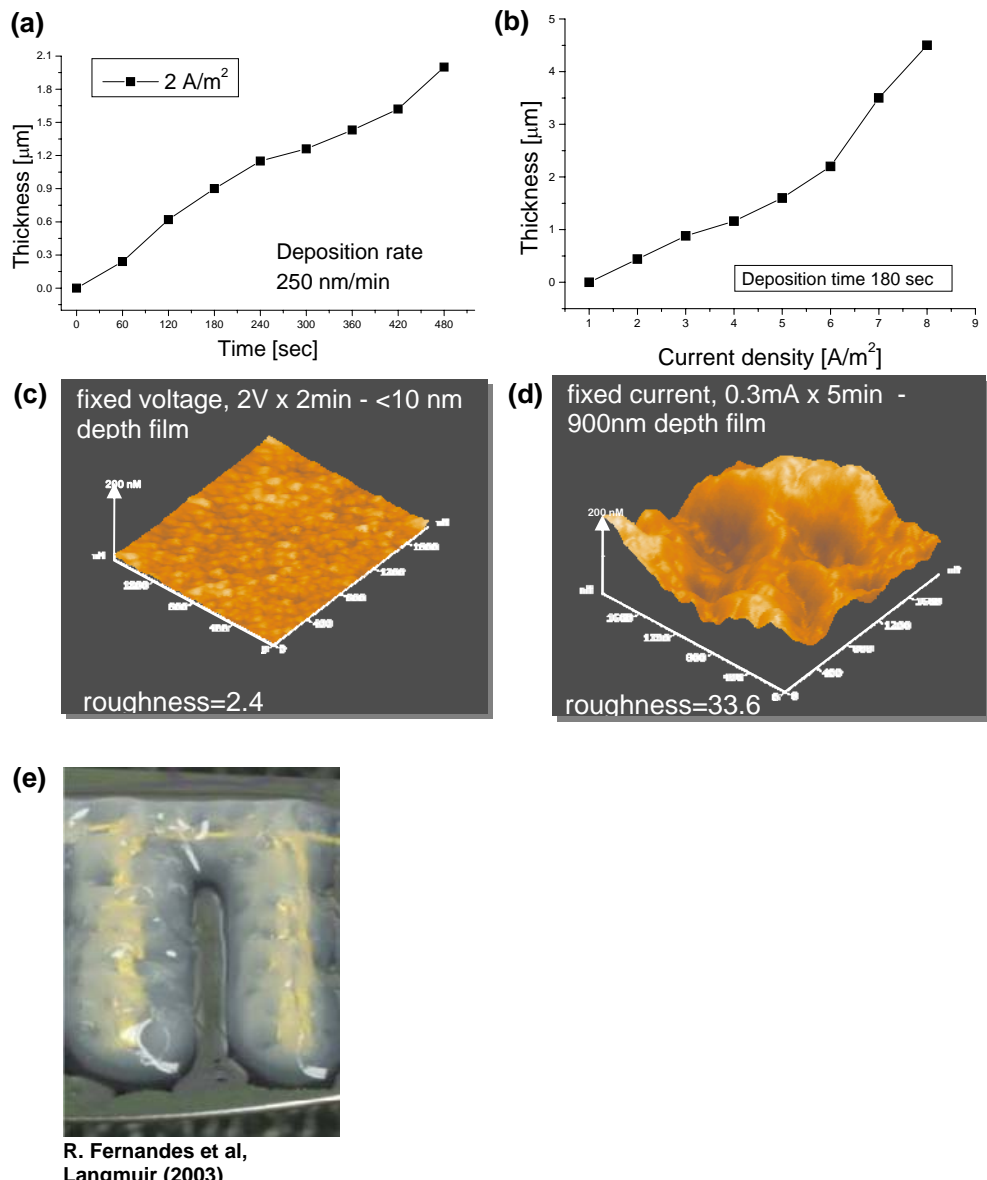


Figure 2-4 (a) Chitosan thickness vs. deposition time (b) Chitosan thickness vs. current density (c) AFM image of chitosan film deposited with constant current (d) AFM image of chitosan film deposited with constant voltage (e) Chitosan hydrogel formation

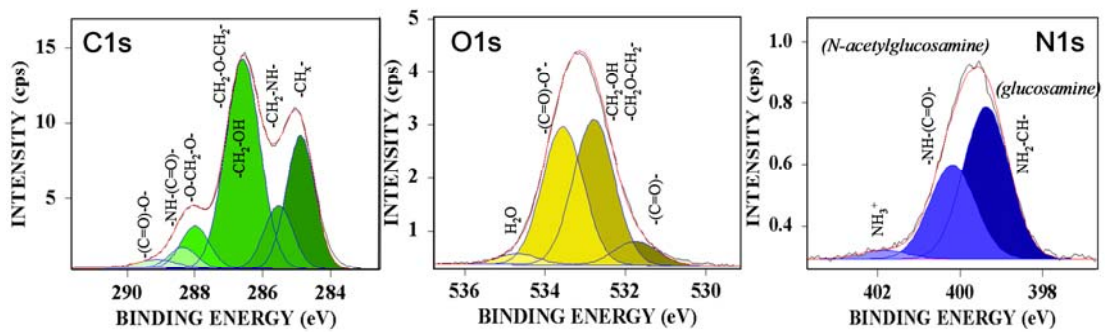


Figure 2-5 XPS analysis on electrodeposited chitosan film surface

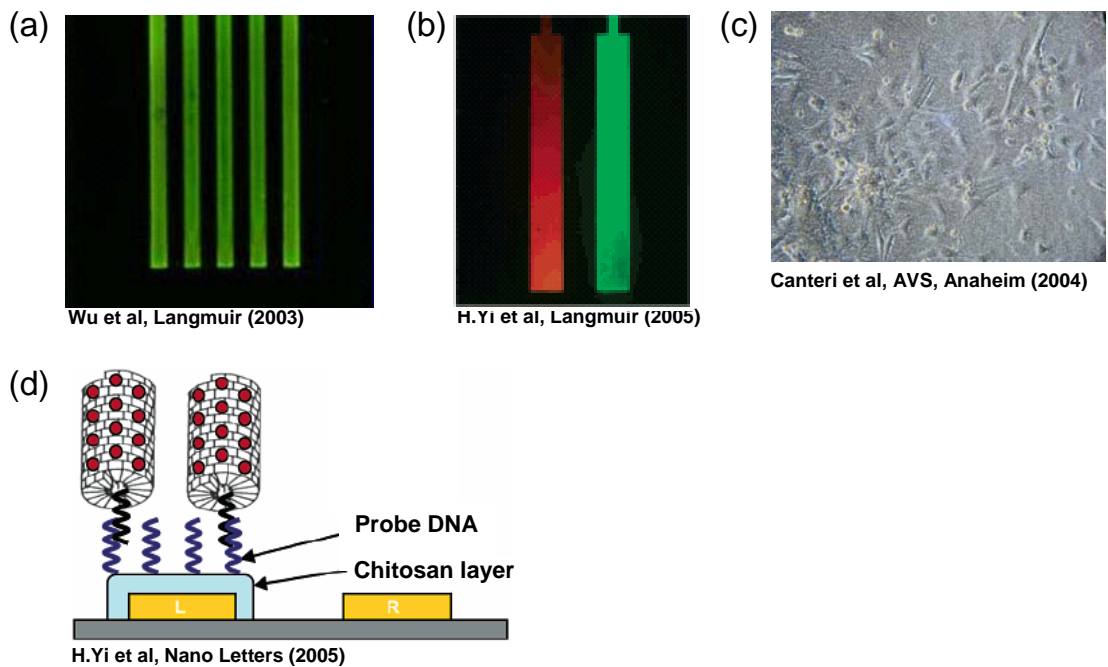


Figure 2-6 (a) Electrodeposited fluorescently labeled chitosan on patterned electrode (b) Chitosan-mediated protein assembly (c) Cell adhesion on chitosan film (d) Schematic drawing of virus assembly on chitosan via DNA cross linker

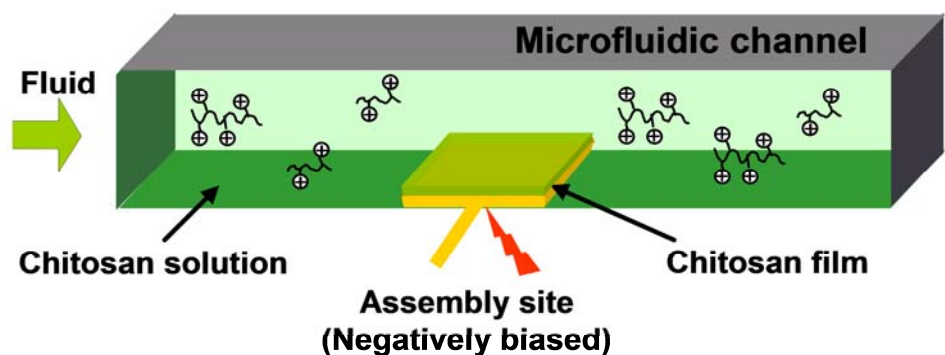


Figure 2-7 Schematic view of chitosan deposition in a microfluidic channel

## **Chapter 3 Novel Wafer Scale Microfluidic System Design and Fabrication**

### **3-1 Microfluidic device wafer design**

To develop a microfluidic device that enables electric signal-guided, post-fabrication biomolecule assembly in a spatially selective manner, we first designed simple networks of microchannels with patterned gold electrodes on a Pyrex wafer as shown in Figure 3.1. Our microfluidic device has several features including all-transparent materials for simple *in situ* microscopic observation of biomolecule assembly events, non-permanent sealing and packaging for further *ex situ* examination of the assembled biomolecules, and flexible PDMS-spun Plexiglas top sealing plate for consistently leak-free sealing. Figure 3.1 (a) shows the design of a microfluidic device wafer composed of 6 identical microchannels, gold electrodes and fluidic and electrical I/Os on a 4" Pyrex substrate. Drilled holes through the Pyrex are provided at the center and around the edge to allow compression system bolts to pass through. Also shown on the right side of Figure 3.1 (a) is a 3-D diagram of a gold electrode, the biomolecule assembly site, inside a microfluidic channel. Figure 3.1 (b) shows a close-up view of one of the fabricated microchannels. Figure 3.1 (c) shows a patterned gold electrode (1mm x 1mm) at the bottom of a microfluidic channel (500  $\mu\text{m}$  wide), which serves as the electric signal-guided biomolecule assembly site. The SU8 microchannel pattern is restricted to a small lateral extent on either side of each microchannel. The SU8 pattern is designed as a micro-knife-edge (400  $\mu\text{m}$  wide, 150  $\mu\text{m}$  deep) to seal the channel by compression action with a PDMS gasket ( $\sim$ 300  $\mu\text{m}$ ). Pyrex satisfies several criteria for the substrate, including

thermal stability at process temperature (~95 °C), resistance to process chemicals, optical transparency, and high electrical resistivity. Similarly, SU8 is effective as the microchannel material because of its chemical, and thermal stability, and because it is readily fabricated with vertical sidewalls and high aspect ratios,<sup>69</sup> properties which have led to its widespread and increasing use as a photoimageable dielectric in lithography for MEMS and bioMEMS applications. Broad range of thickness can be obtained with a conventional spin coater and various features can be patterned on thicker SU8 film (> ~200 μm) with typical UV illumination process.<sup>70</sup> In addition, because SU8 has a higher refractive index than that of both Pyrex and PDMS, it can be used as an optical waveguide when integrated into the SU8 patterns of the microfluidic device wafer, enabling another means for real-time, *in situ* optical analysis of biomolecule assembly in the bioMEMS.<sup>60</sup> This represents an extension of the goal in this work, where our device and packaging design was chosen to enable optical imaging through transparent layers from the top.

### **3-2 Fabrication**

#### **3-2-1 Pyrex substrates for microfluidic device wafer**

There are several ways to create holes in the Pyrex wafer, such as wet/dry etching, laser drilling<sup>71-73</sup> but these methods require long process time and are not cost effective. We adapted a simple drilling method to generate holes on the Pyrex wafer by using silica grit and brass tubing. Before drilling, both sides of the Pyrex wafer (4" diameter, 500 μm thick) were passivated with a photoresist (Shipley 1318) to prevent scratching and to minimize surface contamination during machining processes. Then the Pyrex wafer was

fixed on a  $\frac{1}{2}$ " thick Pyrex plate with a mounting media (Quick-Stick<sup>TM</sup>, Cargille Labs) which is melted at 65 °C on a hot plate. After the cooling process at room temperature,  $\frac{1}{4}$ " diameter holes for the compression bolts were drilled in the 4" Pyrex wafer using a brass tube and 30  $\mu\text{m}$  size of silicon carbide grit (Universal photonics Inc.) in a milling machine. One hole in the center and 6 equally spaced holes around the edge of the wafer on a 1.75" radius were drilled. After drilling, the wafer and the plate were put on a hotplate at 65 °C to melt the mounting media and the wafer was removed from the thick Pyrex plate. Residue of wax and photoresist on the wafer was completely removed with acetone and by immersing in photoresist stripper at 65 °C for 10 min.

### 3-2-2 Gold electrode patterning and SU8 microchannel fabrication

Microfluidic device fabrication process flow is shown in Figure 3-2. First of all, the drilled 4" Pyrex wafer was cleaned with piranha solution ( $\text{H}_2\text{SO}_4:\text{H}_2\text{O}_2 = 3:1$ , for 5 min) before electrode metal deposition. Thin layers of a Cr adhesion layer (90 Å) and then the Au electrode metal (2000 Å) were then deposited on the Pyrex wafer in a sputter deposition system. The wafer was cleaned with acetone, methanol and then finally isopropanol, and dehydrated at 100 °C for 10 min on a hot plate before electrode patterning. Drilled holes are covered with scotch tape prior to photoresist spin to prevent non uniform photoresist spin. Photoresist was then spun onto the wafer and patterned with the electrode mask using contact photolithography.<sup>64</sup> After another cleaning process as described above, SU8-50 (MicroChem, Newton, MA) was spun on the wafer. To avoid the severe non-uniformity in SU8 film thickness which occurred near the drilled holes in the Pyrex wafer, we attached scotch tape on the backside of the drilled hole,

filled the holes with SU8 solution using a pipette, and baked the structure for 60 min at 95 °C to harden the SU8 inside the drilled holes. Then an SU8 film was spun onto the Pyrex wafer using a spin speed of 1,000 rpm for 15 sec (achieving an SU8 thickness ~150 µm), which was followed by a soft baking process at 95 °C for 60 min. SU8 microchannels were patterned using a transparency mask in a UV aligner (1000 mJ/cm<sup>2</sup>, 405 nm UV line), followed by a post baking process at 95 °C for 30 min. Finally, the SU8 film was developed in SU8 developer (MicroChem) for 25 min. The thickness of SU8 film was measured by a mechanical profilometer (Dektak 6M, Veeco Instruments Inc), which showed 10 % thickness variation across the wafer.

### **3-3 Design and Fabrication of Microfluidic Package**

To package the 4" OD Pyrex substrate, the 4 Plexiglas pieces were outfitted with through holes for compression bolts as well as fluidic I/O lines and electrical feedthroughs drilled at the assigned locations.[Figure 3-3] Plexiglas was chosen as packaging material since it is transparent, machinable, inexpensive, and resistant to scratches. After the machining process, a PDMS (Sylgard 184, Dow Corning) gasket film (~300 µm thick) was spun on a top sealing plate. A cork borer was used to punch holes in the PDMS film for fluidic and electrical feedthroughs because the PDMS film covers the drilled holes in the top sealing plate. The fluidic I/O's were made leak-tight using O-rings (Buna-N 004) inserted between top compression plate and top sealing plate, together with fluidic connectors (Nanoport<sup>TM</sup>) bonded to the top compression plate with adhesives. Pogo pins (Interconnect Devices, Inc.) for electrical connection to the gold electrodes were inserted through the electrical feedthroughs. Socket head cap screws

( $\frac{1}{4}$ "-28) and socket set screws (4-40) were used as compression bolts and force tunable screws respectively, with the latter provided to fine tune the stress distribution applied by the top compression plate to the top sealing plate to optimize SU8/PDMS sealing at the micro-knife-edges. Figure 3-4 shows a schematic view of the device packaging process to achieve non-permanent, consistently leak free sealing. First, the PDMS-spun top sealing plate is placed on top of the microchannel wafer. Additional top and bottom Plexiglas plates as well as a top Plexiglas ring with fluidic and electrical ports are then placed and sealed with pressure-adjustable compression bolts at the center and the periphery, and additional set screws. 3-D image of the exploded packaging system and side view of the system are shown in Figure 3-5 (a) and (b). Figure 3-5(b) shows a schematic side view of the Plexiglas microfluidics package, which compresses the microfluidic seals at the SU8/PDMS micro-knife-edge contacts and simultaneously provides fluidic and electrical I/O connections from the device wafer through the package to the outside world. The top sealing plate with PDMS thin film gasket attached is inverted and placed on the Pyrex wafer with SU8 microchannels, so that the PDMS and SU8 are in contact for sealing. The small lateral extent of the SU8 microchannel walls form a micro-knife-edge that concentrates stress in the PDMS gasket layer when the top sealing plate and Pyrex wafer are pressed together. Force-tunable set screws and O-ring seals for the fluidic I/O's in the top compression plate complete the fluidic sealing of the system. In turn, this is accomplished by bolting together the top and bottom compression plates at sites on the periphery and at the center of the wafer. As shown in Figure 3-6, all of the materials of the packaging system are made of transparent materials and height of the packaging system is thin enough ( $\sim 0.8$ ") to enable real-time observations using an

optical or fluorescence microscope.[Figure 3-6 (c)] The completed device has microtubings for fluid transport and electrical input/output connections for signal-guided biomolecule assembly connected to the device.

### **3-4 Non-permanent compression sealing and leak test**

To show compression sealing technology, schematic cross sectional view of the microfluidic channel is shown in Figure 3-7. A flexible thin film PDMS gasket layer spun on the top sealing plate is pressed against the top of the SU8 sidewalls, which act as “micro-knife-edges” that locally deform the PDMS to make a leak-tight seal. To evaluate the performance of the micro-knife-edge sealing technique and the overall microfluidic device and packaging design with regard to fluid leakage, we used water visualized by the presence of colored dye solution, as shown in Figure 3-8. A close-up view of one of the microfluidic channels [Figure 3-8 (a)] with blue dye solution in the channel shows ①well-defined channel structure, ②two gold electrode sites at the bottom of the channel and connected to the I/O port, ③all-transparent materials for *in situ* optical examination and ④leak-free sealing. Micrographs also confirm that our compression sealing technology successfully achieved leak tight fluidic sealing with SU8 microchannel and PDMS layer.[Figure 3-8 (b) and (c)] As shown in the schematic diagram of Figure 3-7, the consistent leak-free sealing of the microfluidic channel is achieved by partial deformation of the thin, flexible PDMS layer spun onto the top sealing plate through compression bolts with well-controlled pressure. Importantly, repeated disassembly/assembly of the packaged device with leak tests using the dye solution showed consistent leak-free sealing with no sign of deterioration, suggesting the

robustness of our sealing strategy.

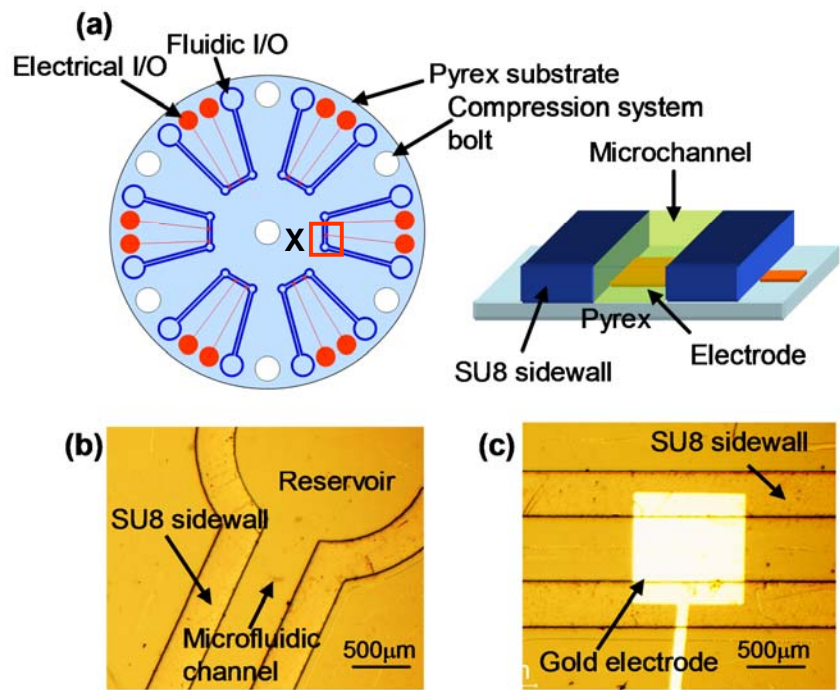


Figure 3-1 (a) Design of microfluidic device wafer and 3-D view of test site X (b) Optical microscopy image of SU8 sidewall and microfluidic channel (c) Magnified image of patterned gold (1mm x 1mm) underneath SU8 microfluidic channel

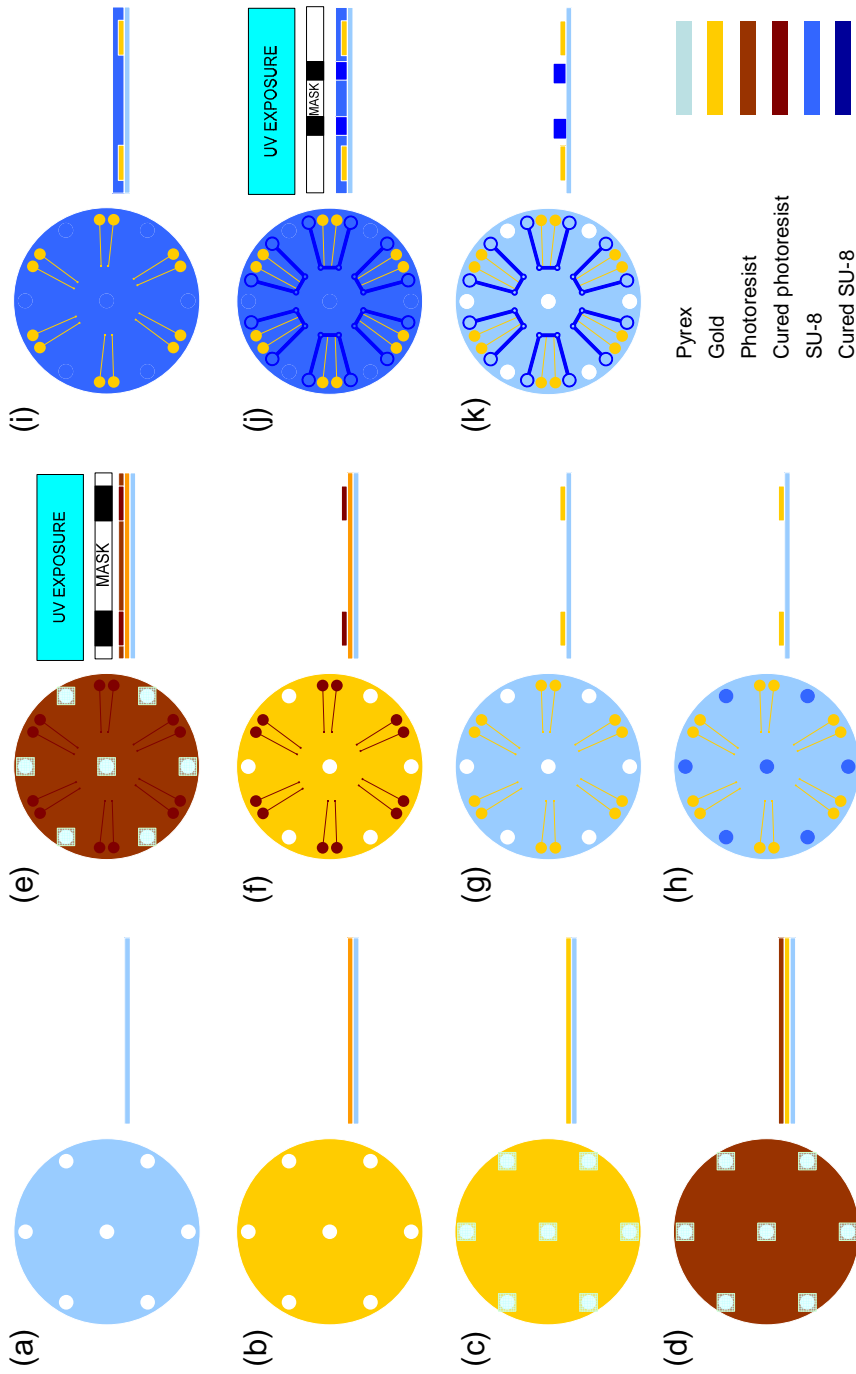


Figure 3-2 Microfluidic device wafer fabrication process flow

(a) 4" Pyrex wafer with drilled holes (b) 2000Å gold deposition (c) Holes covered with scotch tape (d) Photoresist spin (e) UV exposure (f) Photoresist developing (g) Gold etching and photoresist removal (h) Holes are filled with SU8 and SU8 is hardened at 95°C for 60 min (i) 150  $\mu\text{m}$  thick SU8 spun on the wafer (j) UV exposure (k) SU8 developing

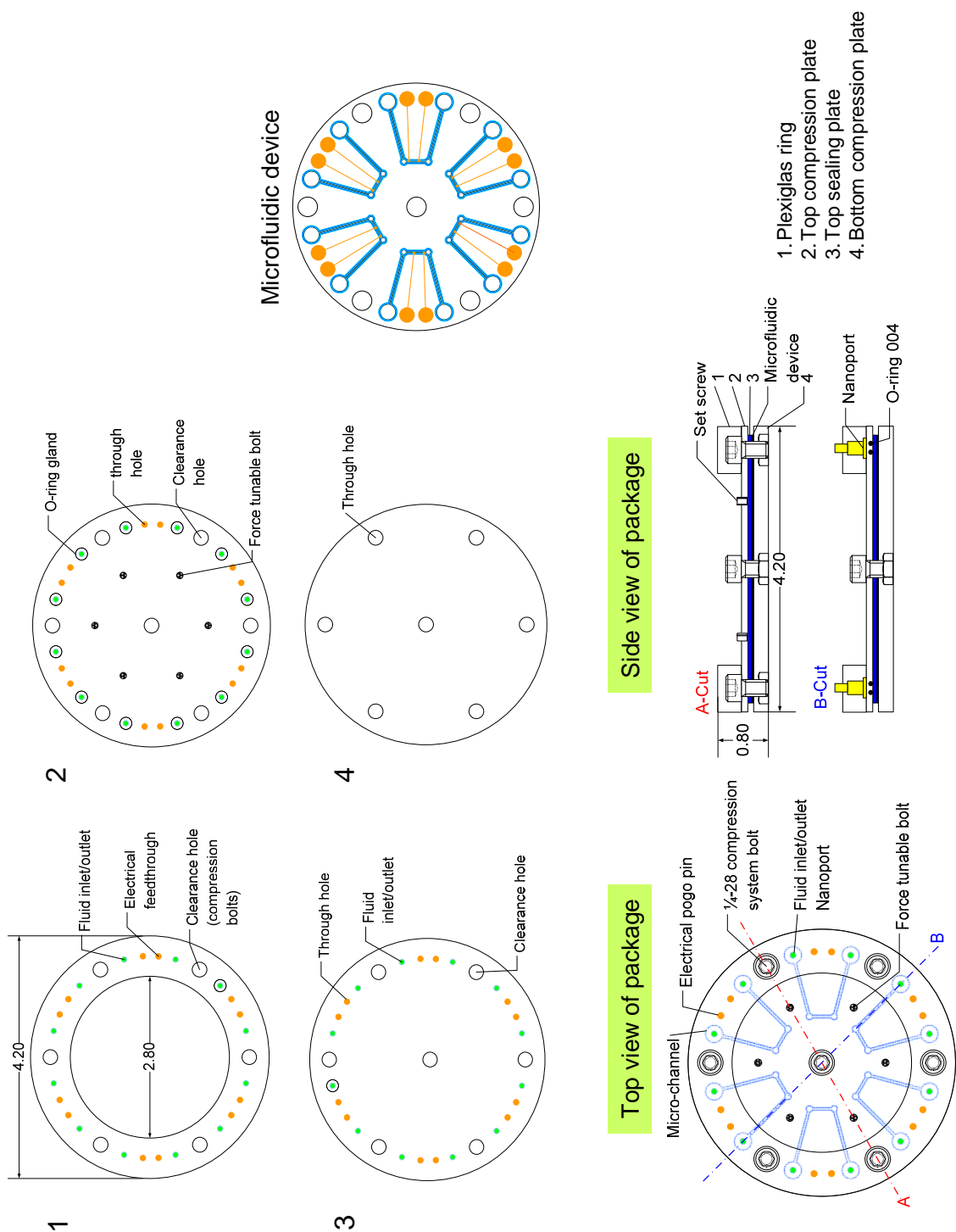


Figure 3-3 Plexiglas package design

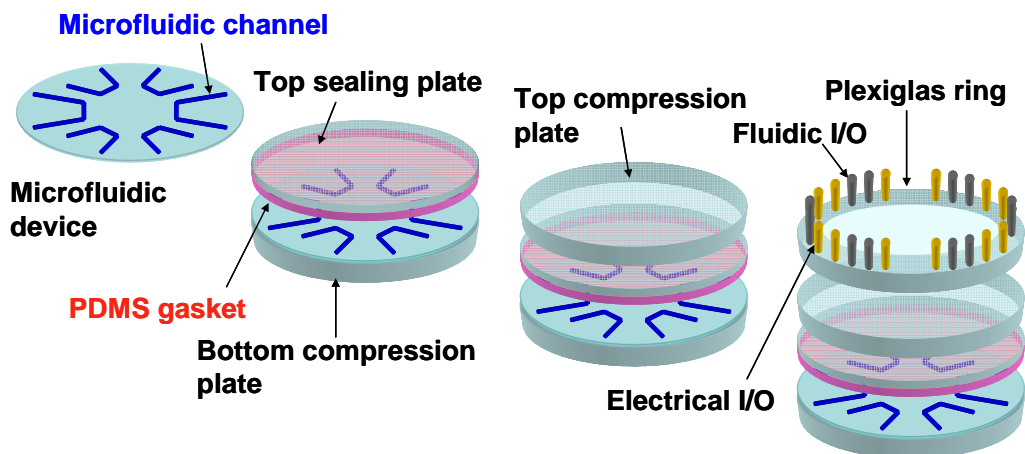


Figure 3-4 Schematic view of microfluidic device packaging process

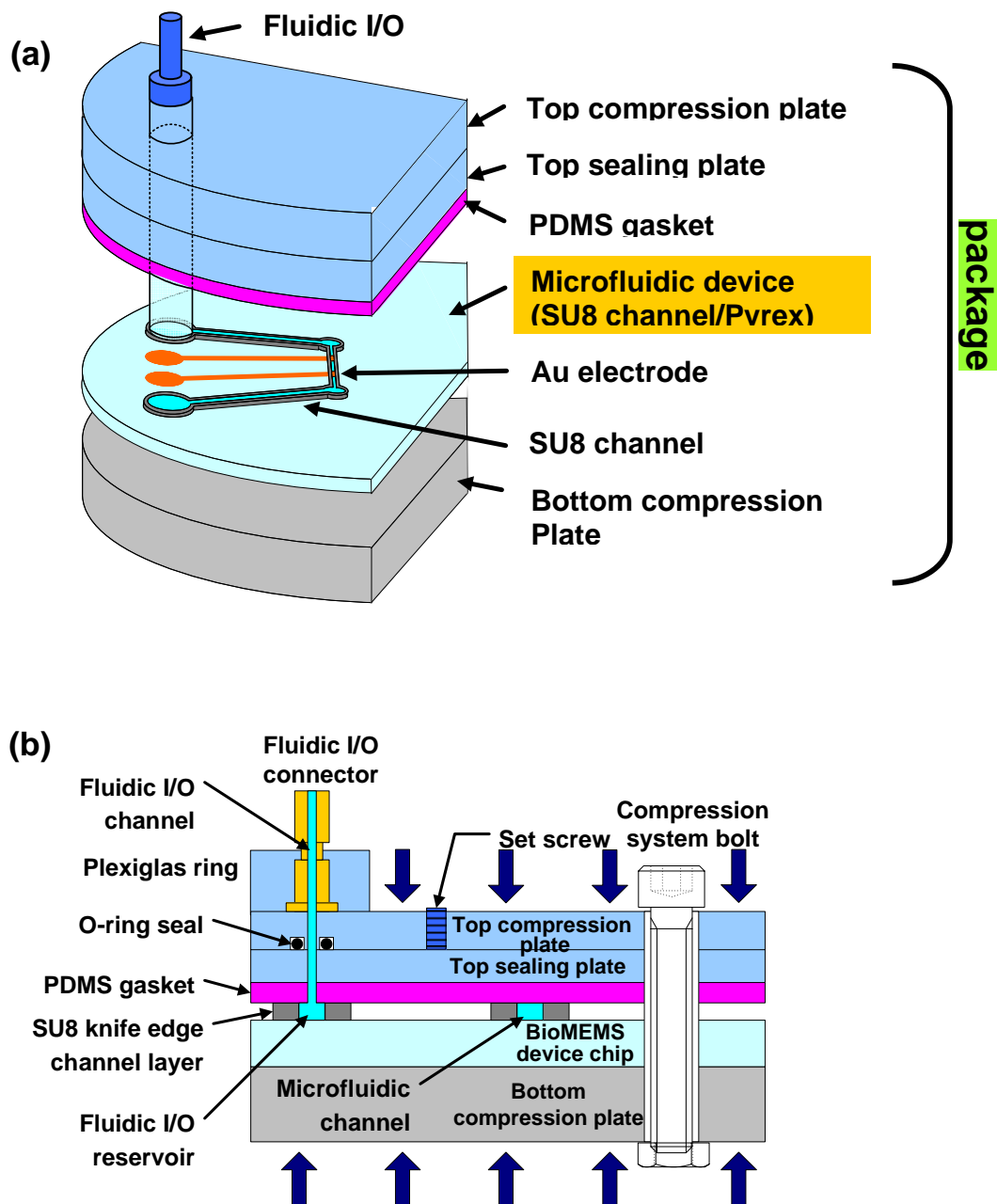


Figure 3-5 (a) Exploded view of the packaging system (b) Schematic side view of microfluidic package

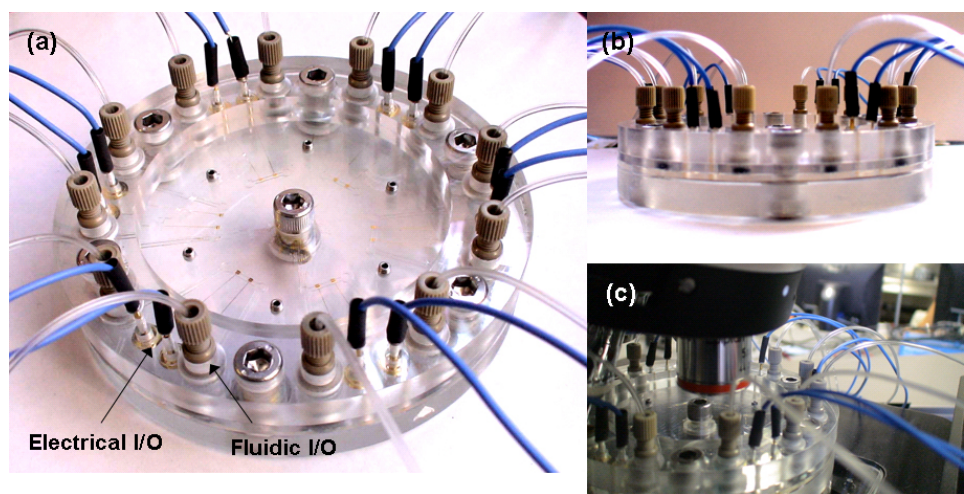


Figure 3-6 (a) Plexiglas microfluidic package for microfluidic device wafer (b) Side view of Plexiglas microfluidic package (c) Microfluidic system under a microscope

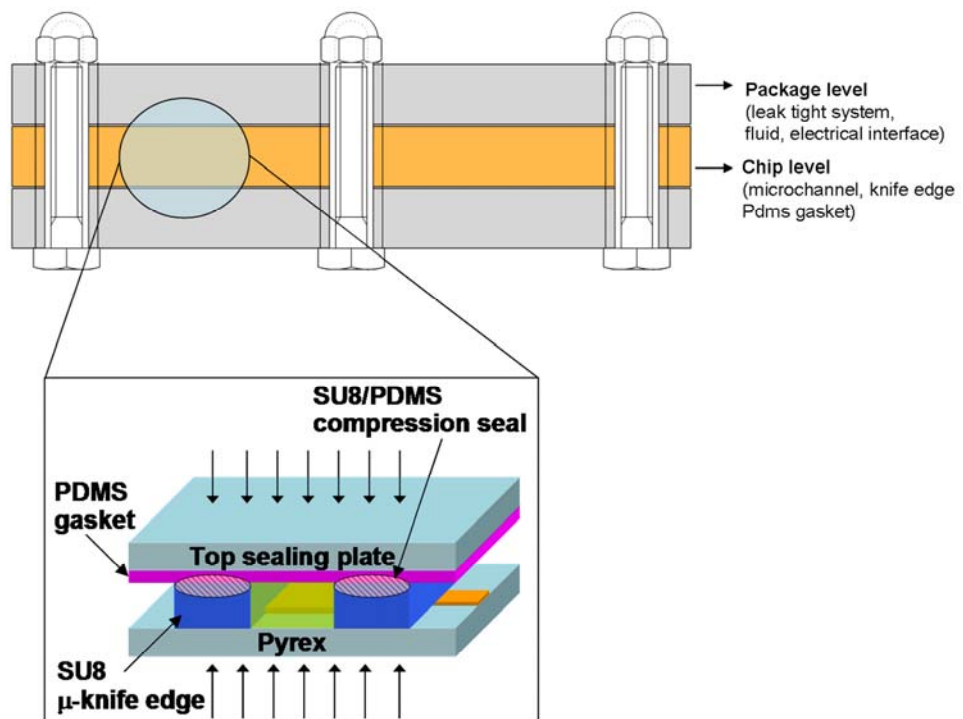


Figure 3-7 Schematic view of microfluidic compression sealing

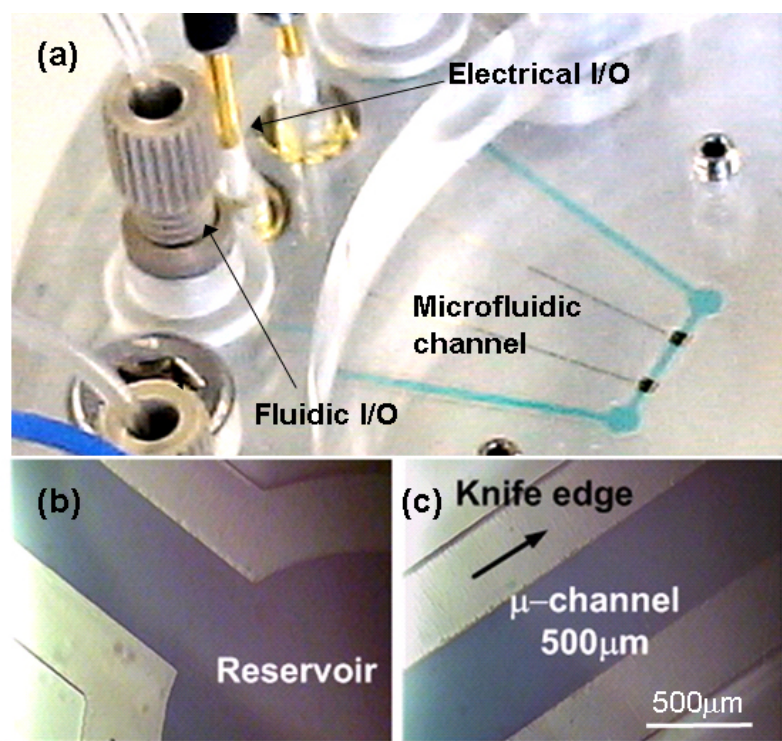


Figure 3-8 (a) Magnified image of microfluidic system with blue dye solution inside the channel (b)-(c) Microscope image of fluid inside reservoir and microfluidic channel

## **Chapter 4 *In situ* chitosan electrodeposition in completely packaged microfluidic devices**

### **4-1 Overview**

We demonstrate the post-fabrication, *in situ* biomolecule assembly approach using the electrodeposition of fluorescently labeled chitosan biopolymer at an internal electrode of a corresponding microfluidic device. Chitosan is an aminopolysaccharide with unique pH-responsive properties that can be harnessed to assemble biological molecules onto inorganic surfaces. Each glucosamine monomer unit of chitosan has a primary amine group with a low pKa value ( $\approx 6.3$ ), which is protonated and positively charged at low pH. These amine groups become deprotonated and neutral as pH increases. This pH-responsive property allows spatially selective assembly of chitosan onto a negatively charged electrode surface.<sup>56, 57</sup> Further, this primary amine group is nucleophilic at neutral state thus allowing various amine group reactive chemistries to be used for covalent conjugation of biomolecules onto chitosan. A wide variety of biomolecules (proteins, enzymes, DNA, RNA) can then be assembled onto this electrodeposited chitosan.<sup>55, 58, 59</sup> In this work, we use fluorescently labeled chitosan to directly demonstrate biomolecule assembly at specific electrodes inside a microfluidic channel within the completely packaged microfluidic device, indicating the potential of this platform for biomolecular reaction processes. As a next set of experiment, we demonstrate electrodeposition of chitosan film in the microchannel by sequentially assembling fluorescent marker molecules, fluorescein, onto electrodeposited unlabeled chitosan scaffold, illustrating electric signal-guided *in situ* biomolecule assembly at

readily addressable sites in the microfluidic channels. Experimental set up for the chitosan deposition in microfluidic system is shown in Figure 4-1. The external micropump is operated by LabView based fluidic control system to control flow in more precise manner and importantly it will allow multiple bioreaction process steps in a complex fluidic network.

## 4-2 Experimental condition

### 4-2-1 Electrodeposition of fluorescein labeled chitosan film

Schematic process flow of electrodeposition of fluorescently labeled chitosan inside a microchannel is shown in Figure 4-2. First, fluorescently labeled chitosan solution (0.5 % (w/v), pH ~ 5) was prepared for the deposition in a microfluidic system.<sup>56</sup> The chitosan solution was introduced through a tubing (0.19 mm ID, Tygon<sup>®</sup>) into the microfluidic system by a micropump (Masterflex<sup>®</sup> pump drive, Cole-Palmer Instrument Co) with a flow rate of 5 µl/min. After the microchannel with two electrodes at the channel bottom was completely filled with chitosan solution, the pump was stopped and a constant current signal of 2 A/m<sup>2</sup> by a power supply (Keithely 2400 source meter) was applied for 4 minutes to electrodeposit chitosan onto the negatively biased working electrode. LabView control software was used to control the chitosan electrodeposition process and to monitor the voltage of the applied electrical signal, which showed 2~3 volts during the electrodeposition process. Then the pump was switched on again to drain chitosan solution and DI water was provided to rinse out excessive chitosan molecules loosely attached on the deposited chitosan film. For real-time, *in situ*

fluorescence observation of the localized chitosan electrodeposition, the microfluidic device was placed under a microscope (Zeiss model 310) equipped with a UV source (Zeiss HBO 100) equipped with a filter set matched to NHS-fluorescein (excitation band 490-495 nm, emission band 520-525 nm). Photomicrographs were prepared from the microscope using a digital camera (Carl Ziess AxioCam MRc5).

#### 4-2-2 Fluorescent labeling of electrodeposited chitosan film

To avoid cross contamination between the several solutions, we used multiple tubings for each solutions and LabView based fluidic control system was developed to enhance control over multiple solutions and processes. Schematic process flow of fluorescein labeling on electrodeposited chitosan inside a microchannel is shown in Figure 4-3. First, microchannel and tubing were cleaned with distilled water, HCl, and finally distilled water for 30 min, 5min, and 30 min respectively with flow rate of ~ 50  $\mu$ l/min. The chitosan solution (0.375 % (w/v), pH ~ 5) as introduced through a tubing (0.19 mm ID, Tygon<sup>®</sup>) into the microfluidic system by a micropump with a flow rate of 5  $\mu$ l/min. With the pump stopped, chitosan film was deposited on the negatively biased electrode with current density 3 A/m<sup>2</sup> for 240 sec. Then the pump was switched on again to drain chitosan solution and Phosphate Buffered Saline (PBS) buffer (pH ~ 7) was provided to neutralize the deposited chitosan film for 30 min with 5  $\mu$ l/min flow rate. Then we introduced carboxyfluorescein succinimidyl ester (NHS-fluorescein) solution over the deposited chitosan film for 30 min with 5  $\mu$ l/min flow rate. For real-time, *in situ* fluorescence observation and image acquisition of the fluorescent labeling of the electrodeposited chitosan film, the same optical microscopy set up was used as described

above. Finally PBS buffer was provided to rinse the remaining NHS-fluorescein solution in the microchannel. To demonstrate negative control of this experiment, we repeated this experiment with the same process sequence on a separate microchannel of the microfluidic device but voltage was not applied to the electrode. To analyze 3-D contour and profile of fluorescent intensity from fluorescently labeled chitosan, we used ImageJ software (National Institutes of Health). Mechanical profilometer (Veeco, Dektak 6M Stylus Profiler) was used to measure the thickness of the chitosan layer in the microchannel by opening the non-permanently packaged device.

### 4-3 Results

#### 4-3-1 Fluorescently labeled chitosan deposition in microfluidic channels

Chitosan electrodeposition in microfluidic channels at readily addressable assembly sites as shown in Figure 4-4, we demonstrate programmed assembly of biological materials in the microfluidic system through electrodeposition of fluorescently labeled chitosan biopolymer film at a readily addressable electrode site in a microchannel upon completion of the device packaging. Electrolysis of water generates a high pH region on the negatively biased gold electrode surface, which together with the electric field at the surface leads to chitosan layer deposition at this electrode site.<sup>56, 57</sup> As indicated in the schematic drawing in Figure 4-4 (a), the chitosan molecules are protonated in the low pH bulk solution, but become deprotonated as they enter the high pH region near the negative electrode and form biopolymeric hydrogel network at the electrode surface with high spatial resolution. First, fluorescently labeled chitosan solution was introduced into

the microfluidic channel using a micropump. After the microfluidic channel was filled with the solution, the pump was stopped and negative bias (relative to another electrode in the system) was applied to the assembly electrode. The chitosan solution was then drained off and the channel was rinsed with distilled water. As shown in the fluorescence micrograph of Figure 4-4 (b), no significant fluorescence is observed before the chitosan electrodeposition. Upon the electrodeposition of chitosan, Figure 4-4 (c) shows significant fluorescence well confined in the electrode region, illustrating the presence of assembled chitosan layer. Importantly, the assembled chitosan layer was well retained through rinsing procedure, as shown in Figure 4-4 (d). This result indicates that biopolymer chitosan can be assembled at readily addressable sites from the aqueous solution through electric signal. These results also illustrate that biopolymeric material (in this case chitosan) can be assembled in the microfluidic channel after completion of the device fabrication and packaging, and that our non-permanent packaging strategy for transparent devices allows *in situ* examination of the biomolecular assembly sites through fluorescence microscopy and possible *ex situ* analysis on the internal bio-structures assembled inside microchannels.

#### 4-3-2 Fluorescent labeling of electrodeposited chitosan

As shown in Figure 4-5, we then demonstrate conjugation of a fluorescent marker to the electrodeposited chitosan, and further analyze the assembled layer by comparing the fluorescence intensity profile and physical thickness. First, unlabeled chitosan was electrodeposited at the assembly site by introducing chitosan solution into the microchannel and applying negative bias. As shown in Figure 4-5 (a), the unlabeled

chitosan yields no significant fluorescence upon electrodeposition. As shown in Figure 4-5 (b), amine group reactive NHS-fluorescein solution was then introduced into the microchannel. NHS-fluorescein selectively reacts with chitosan's abundant amine groups to form covalent amide linkage, resulting in fluorescent labeling of chitosan.<sup>57</sup> Figure 4-5 (c) shows that only the assembly site was fluorescently labeled, demonstrating the retained chemical reactivity and spatial selectivity of the electrodeposited chitosan layer. This result strongly suggests that electrodeposited chitosan layer can serve as a spatially selective scaffold for post-fabrication, *in situ* covalent conjugation of biological molecules. To confirm that the chitosan is required for such conjugation, we then performed identical sequence of events in a separate microchannel of the microfluidic device, except that no negative voltage was applied to the electrode. As shown in Figure 4-5 (d), the assembly site showed no noticeable fluorescence upon the introduction of chitosan without negative bias and then NHS fluorescein, confirming that the fluorescence shown in Figure 4-5 (c) indeed resulted from conjugation of fluorescein to the electrodeposited chitosan. Next, we analyzed the fluorescence intensity of the labeled chitosan using ImageJ image analysis software, as shown in Figure 4-6 (b) and (c). This 3-D contour profile shows relatively uniform fluorescence along the length of the assembly site with slightly higher intensity around at the electrode edges. It is speculated that higher electric field generated at the edge of the electrode during electrodeposition process causes thicker deposition of chitosan film. Finally, we examined the chitosan layer by disassembling the non-permanently sealed package and by measuring the thickness using a mechanical profilometer. As shown in Figure 4-6 (d), the actual thickness profile showed good agreement with the fluorescence profile (Figure 4-6 (c)),

indicating that the fluorescence profile obtained by *in situ* fluorescence labeling and observation reflected the actual amount of chitosan well. Importantly, this result illustrates that our non-permanent sealing scheme enables simple *ex situ* examination of physical properties that reassures the results obtained by *in situ* optical examination of the assembly and conjugation of biomolecular layer. Combined these results show that electrodeposition of chitosan enables further post-fabrication, *in situ* biomolecular assembly by harnessing the abundant amine groups of chitosan that retained chemical reactivity upon electrodeposition.

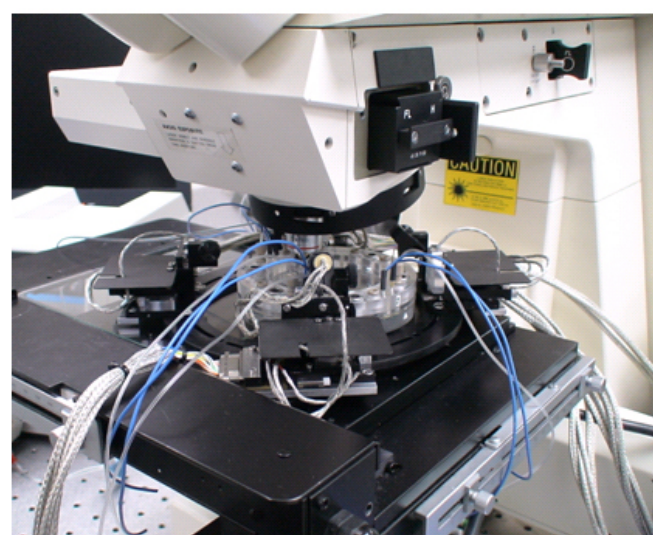
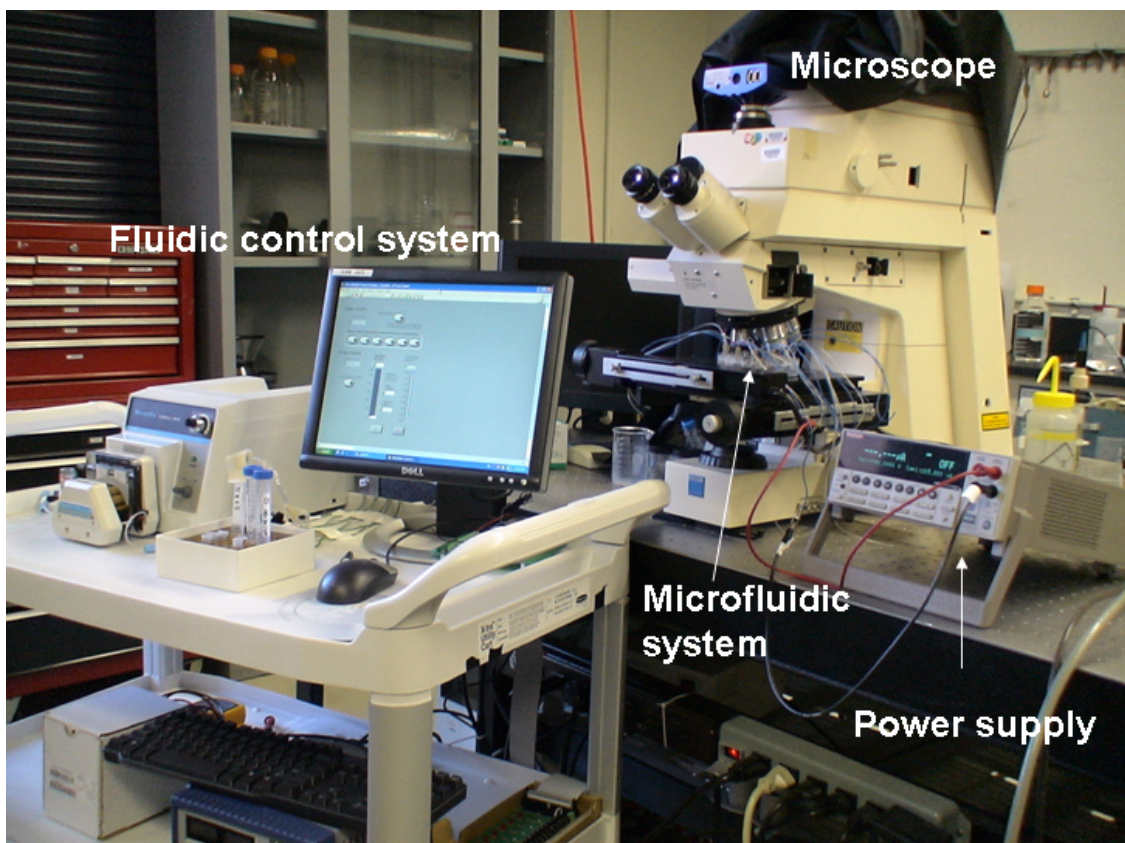
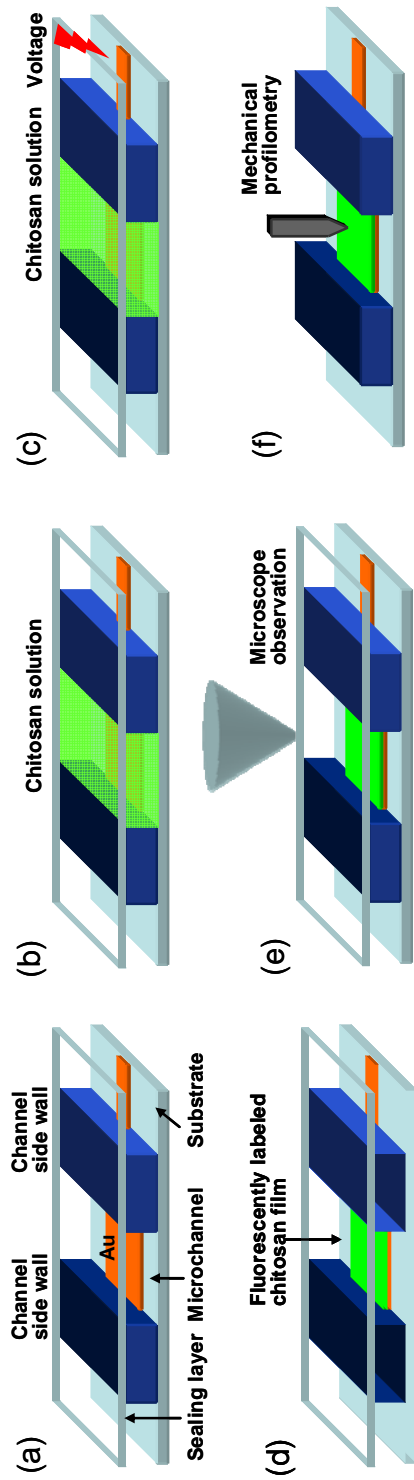
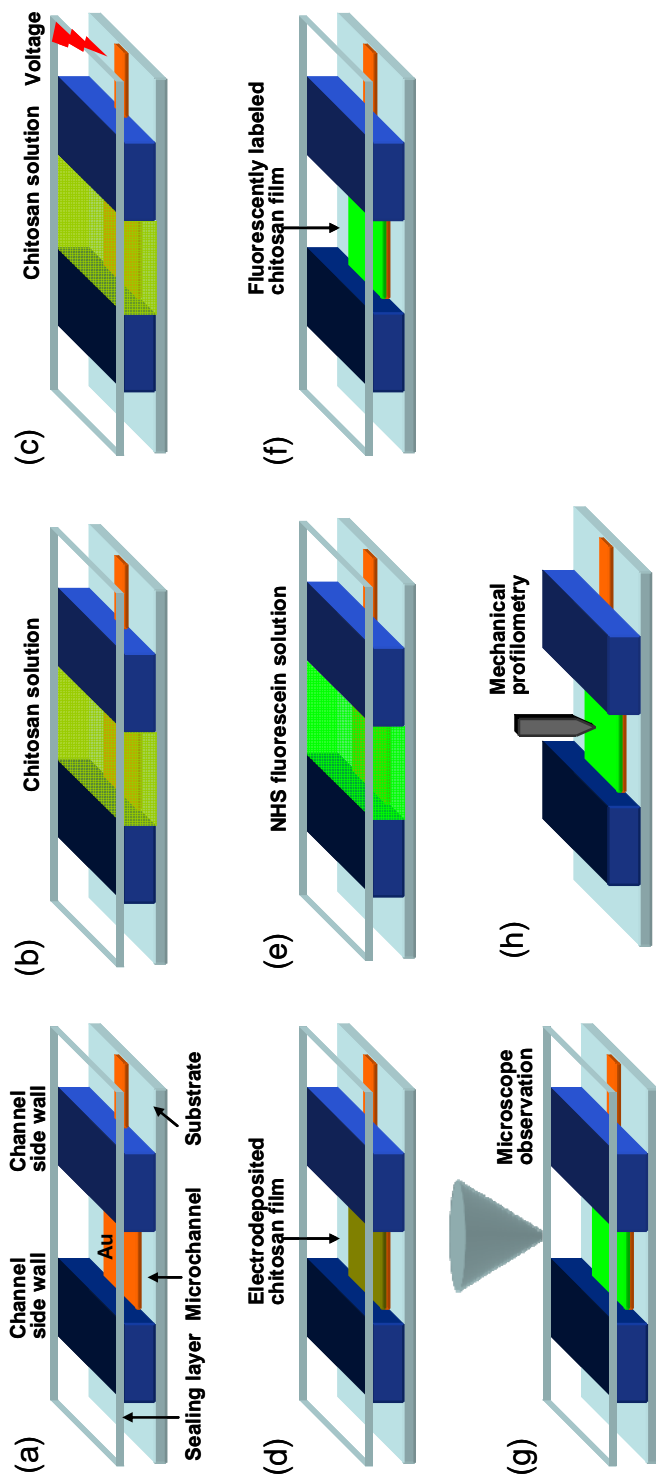


Figure 4-1 (a) Experimental set up for biomolecule assembly in microfluidic system (b) Magnified image of microfluidic system under the microscope



(a) Before chitosan deposition (b) Chitosan solution introduction (c) Electrodeposition of chitosan (d) Fluorescently labeled chitosan film (e) Microscope observation (f) Ex-situ mechanical profilometry on assembly site

Figure 4-2 Schematic process flow of electrodeposition of fluorescently labeled chitosan inside microchannel



(a) Before chitosan deposition (b) Chitosan solution introduction (c) Electrodeposition of chitosan (d) Electrodeposited chitosan film (e) Fluorescent labeling (f) Fluorescently labeled chitosan film (g) Ex-situ mechanical profilometry (h) Microscope observation

Figure 4-3 Schematic process flow of fluorescent labeling of electrodeposited chitosan inside microchannels

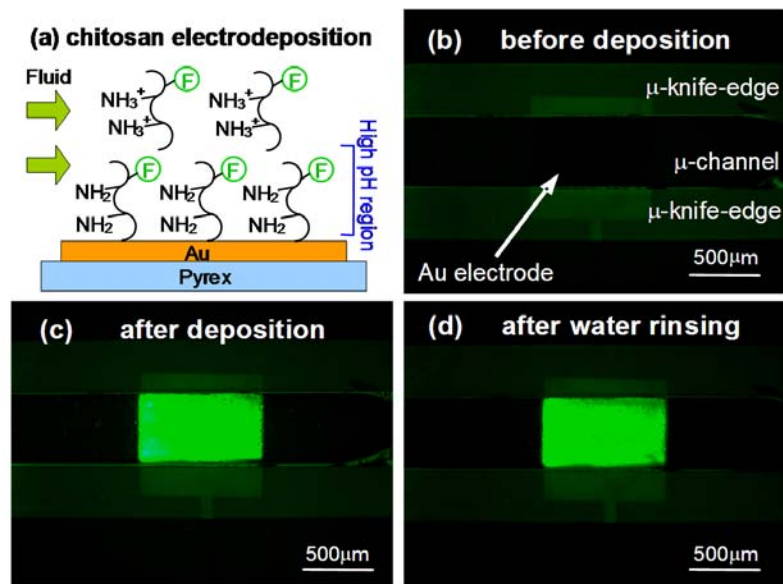


Figure 4-4 (a) Schematic drawing of chitosan electrodeposition at the negatively biased electrode in the microfluidic channel (b-d) Fluorescence micrographs of the assembly site in microchannel (b) Before deposition, (c) After deposition, (d) After final water rinsing. Chitosan deposition was carried out at  $2\text{A/m}^2$  for 240 sec.

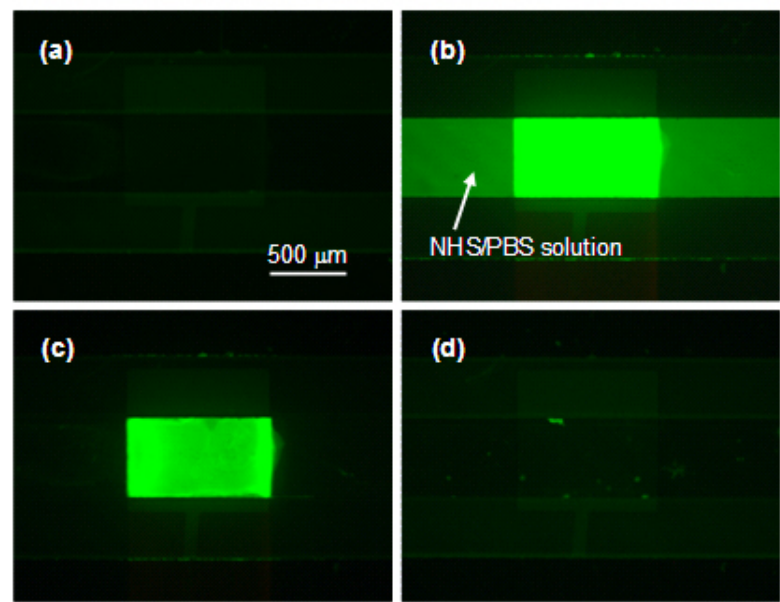


Figure 4-5 (a) After chitosan deposition (b) NHS-fluorescein solution filled in the microfluidic channel (c) After labeling reaction (d) Negative control channel (no bias)

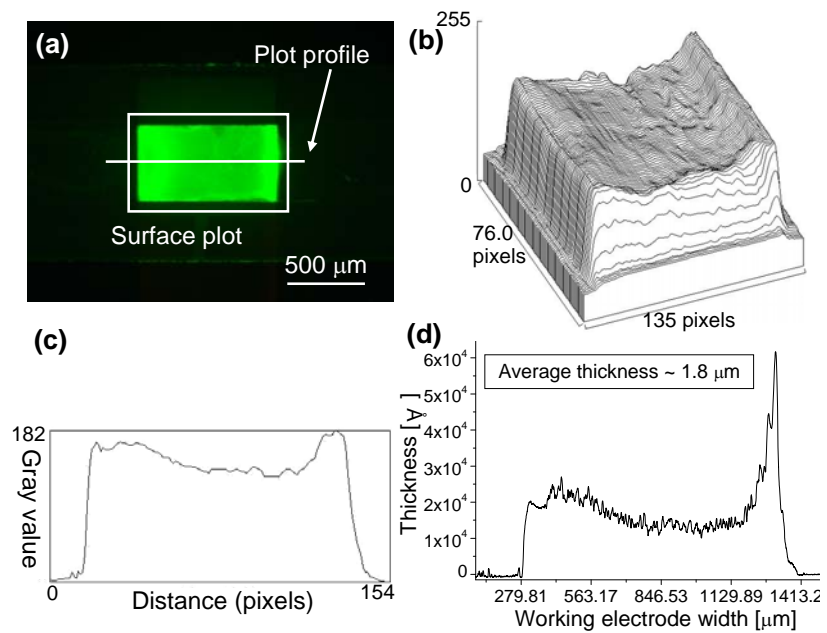


Figure 4-6 (a) Fluorescently labeled chitosan film showing the areas/sections for fluorescence profile analyses (b) Image J surface plot (c) Image J plot profile (d) Thickness by mechanical profilometry

## **Chapter 5 Chitosan-mediated *in situ* biomolecular assembly in completely packaged microfluidic devices**

### **5-1 Overview**

We demonstrate facile chitosan-mediated *in situ* biomolecule assembly at readily addressable sites in microfluidic channels after complete fabrication and packaging of the microfluidic system. Recently the patterning of biomolecules onto substrates is of great interest. DNA or protein based bioMEMS are used for wide variety of applications (genomics, proteomics or biosensors, biosynthesis, biochemical analysis) due to high selectivity of biomolecules and advantage of microscale environment.<sup>9-13</sup>

Aminopolysaccharide chitosan's pH responsive and chemically reactive properties allow electric signal-guided biomolecule assembly onto conductive inorganic surfaces from the aqueous environment, preserving the activity of the biomolecules. A wide variety of biomolecules (proteins, DNA, RNA, enzymes) can then be assembled onto this electrodeposited chitosan by covalent conjugation to the amine group of each glucosamine monomer unit of chitosan. In this work, we demonstrate GFP (green fluorescent protein) assembly onto electrodeposited chitosan scaffold to directly show biomolecule assembly at specific electrodes inside a microfluidic channel within the completely packaged microfluidic device, indicating the potential of this platform for biomolecular reaction processes. First unlabeled chitosan film is electrodeposited in the microchannel, followed by glutaraldehyde, an amine group reactive homobifunctional crosslinker, activation process. GFP is then introduced into the microchannel and assembled on the chitosan scaffold via glutaraldehyde crosslinking agent.

As a next set of experiment, we demonstrate biomolecule assembly on chitosan film in the microchannel by assembling probe DNA onto electrodeposited unlabeled chitosan scaffold via glutaraldehyde and subsequent hybridization of match target DNA on the probe DNA, indicating signal-guided sequential assembly of nucleic acids onto readily addressable sites in the microchannel. First unlabeled chitosan film is electrodeposited in the microchannel, followed by glutaraldehyde, crosslinker, activation process. Probe DNA is then introduced into the microchannel and assembled on the chitosan scaffold via glutaraldehyde crosslinking agent. Then match target DNA is introduced and hybridized with the probe DNA assembled on the chitosan scaffold.

Transparent and non-permanently packaged device allows consistently leak-free sealing, simple *in situ* and *ex situ* examination of the assembly procedures, fluidic input/outputs for transport of aqueous solutions, and electrical ports to guide the assembly onto the patterned gold electrode sites within the channel. Both *in situ* fluorescence and *ex situ* profilometer results confirm chitosan-mediated *in situ* biomolecule assembly, demonstrating a simple approach to direct the assembly of biological components into a completely fabricated device. We believe that this strategy holds significant potential as a simple and generic biomolecule assembly approach for future applications in complex biomolecular or biosensing analyses as well as in sophisticated microfluidic networks.

## 5-2 Experimental condition

### 5-1-1 GFP assembly on electrodeposited chitosan film

We deposited unlabeled chitosan film inside microchannel and Green Fluorescent Protein (GFP) was assembled onto the chitosan film via glutaraldehyde crosslinking reagent. Figure 5-1 shows a schematic process flow of GFP assembly on electrodeposited chitosan scaffold inside a microchannel. First same cleaning steps, chitosan deposition process, and PBS buffer neutralization steps were performed as described in the previous chapter. Glutaraldehyde solution (0.5 %) was then introduced at 5  $\mu$ l/min for 30 min, followed by PBS buffer rinsing for 30 min. GFP solution was then flowed in the microfluidic channels for 15 min with 5  $\mu$ l/min flow rate. For *In situ*, real time observation on the test site, microfluidic system was placed under the microscope during whole process step as shown in Figure 4-1. Finally, the microfluidic channel was rinsed with 5  $\mu$ l/min PBS for 30 min. For the negative control, we repeated the same processes on a separate channel of the microfluidic device except that no negative bias was applied to the electrode. ImageJ analysis software and mechanical profilometer were used to analyze fluorescent 3-D contour and internal bio-structure inside the microchannel.

### 5-2-2 DNA assembly/hybridization in microfluidic system

We deposited unlabeled chitosan film inside the microchannel and probe DNA was assembled onto the deposited chitosan film via glutaraldehyde crosslinking agent. Subsequently target DNA was introduced into the microchannel and hybridized with the probe DNA assembled on the chitosan film. Schematic process flow of DNA hybridization on electrodeposited chitosan scaffold inside a microchannel is shown in

Figure 5-2. First same cleaning steps, chitosan deposition process, and PBS buffer neutralization steps were performed as described above. Glutaraldehyde solution (0.5 %) was then introduced at 5  $\mu$ l/min for 30 min, followed by PBS buffer rinsing for 30 min. Probe DNA solution (20  $\mu$ g/ml) was introduced over the activated chitosan in the microchannel for 60 min with 5  $\mu$ l/min flow rate, followed by PBS buffer rinsing for 30 min. NaBH4 solution, PBS buffer and hybridization buffer were then introduced into the microchannel in sequence for 20 min, 30 min and 10 min respectively. For the DNA hybridization step, firstly, mismatch target DNA (0.5  $\mu$ M in hybridization buffer) was flowed over the probe DNA assembled chitosan film at the assembly site in the microchannel for 30 min with 5  $\mu$ l/min flow rate, followed by hybridization buffer conditioning for 10 min. Then match target DNA (0.5  $\mu$ M in hybridization buffer) was then introduced into the microchannel for 30 min with 5  $\mu$ l/min flow rate, followed by hybridization buffer and PBS buffer rinsing for 10 min respectively. For *in situ*, real time observation on the test site, microfluidic system was placed under the microscope during whole process steps. ImageJ analysis software and *ex-situ* mechanical profilometer were used to analyze fluorescent 3-D contour and internal bio-structure.

### 5-3 Result

5-3-1 Post-fabrication *in situ* GFP assembly onto electrodeposited chitosan scaffold in the microfluidic channels

Finally, we demonstrate *in situ* GFP (green fluorescent protein) assembly onto

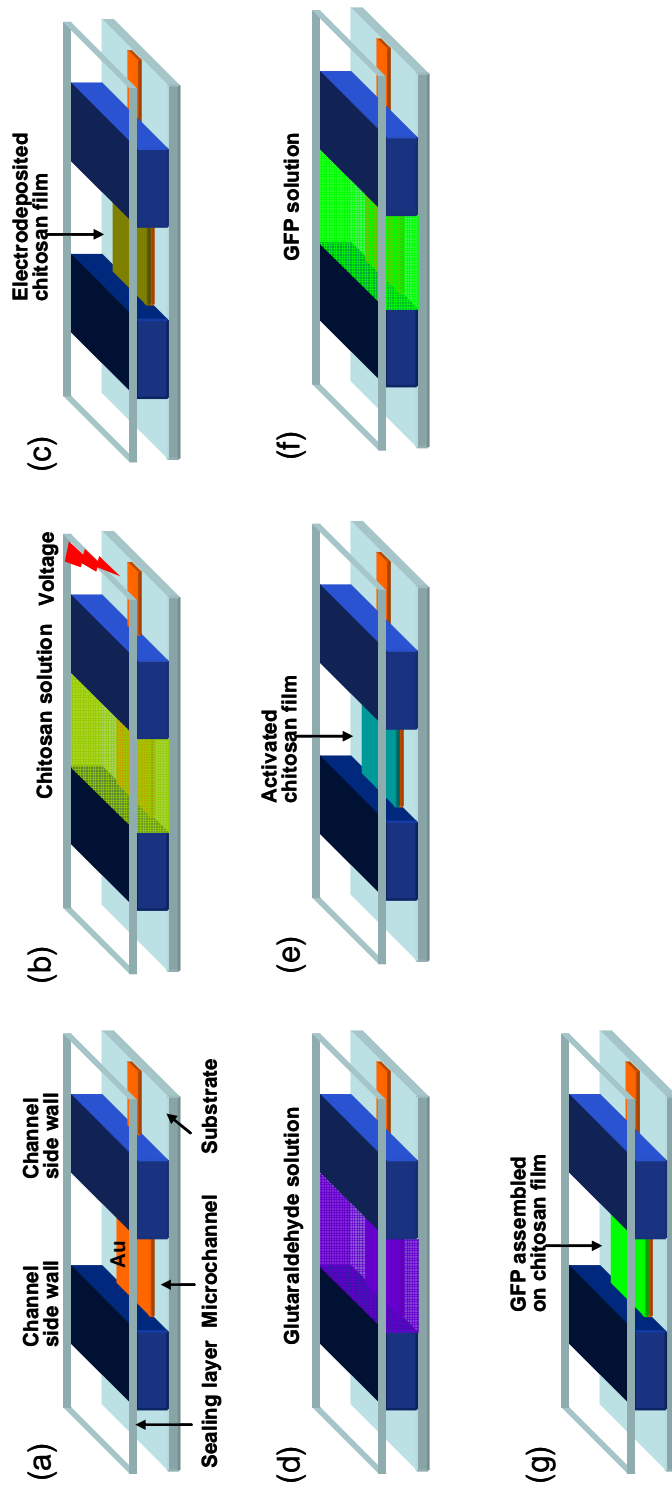
electrodeposited chitosan scaffold through a chemical crosslinking reagent in the microfluidic channel, as shown in Figure 5-3. For this, we reassembled the microfluidic system after the profilometer measurement [Figure 4-6 (d)], and electrodeposited chitosan at a separate microfluidic channel on the same microfluidic device. Then we introduced 0.5% aqueous solution of glutaraldehyde, an amine group reactive homobifunctional crosslinker that activates chitosan for covalent coupling with amine groups on proteins. As shown in Figure 5-3 (a) and (b), no significant fluorescence appears up to chitosan electrodeposition and the glutaraldehyde activation step as expected. Next, we introduce aqueous solution of GFP into the microchannel. Figure 5-3 (c) illustrates that GFP reacts with and becomes conjugated onto the activated chitosan scaffold. This result shows that electrodeposited chitosan enables post-fabrication, *in situ* assembly of proteins in microfluidic channels through series of simple standard chemical reactions all in aqueous environment. Importantly, the assembled GFP retains the fluorescence (Figure 5-3 (c)), indicating that the structure of the protein is preserved throughout the assembly procedure. In contrast, Figure 5-3 (d) shows a negative control channel, which underwent the identical procedure as the previous channel except that the electrode was not negatively biased for chitosan electrodeposition. This result reconfirms that the *in situ* protein assembly requires electrodeposited chitosan as the covalent coupling scaffold. Further, fluorescence profile analysis was performed on the assembly site (Figure 5-3 (e)) and 3-D fluorescent contour shows uniform fluorescent intensity of GFP decorated chitosan film (Figure 5-3 (f)). Combined these results demonstrate *in situ* protein assembly in the microfluidic device, which could further be exploited for biochemical reactions or biosensing applications based on *in situ* assembled enzymes or

antibodies at readily addressable, activated chitosan scaffold sites in microfluidic devices. Particularly important to note is that the sequences of steps and electric signal-guided biomolecule assembly strategy allow all-aqueous environment for the protein assembly, preserving the biological activities.

### 5-3-2 *In situ* probe DNA assembly onto electrodeposited chitosan scaffold and match target DNA hybridization in the microfluidic channels

We demonstrate *in situ* probe DNA assembly onto electrodeposited chitosan scaffold through a chemical crosslinking reagent in the microfluidic channel and subsequently target DNA is introduced and hybridized on the assembled probe DNA, as shown in Figure 5-4. For this, we electrodeposited chitosan film at a separate microfluidic channel of the same microfluidic device. Then we introduced 0.5% aqueous solution of glutaraldehyde, an amine group reactive homobifunctional crosslinker that activates chitosan film for covalent coupling with amine groups of the probe DNA. As shown in Figure 5-4 (a) and (c), no significant fluorescence was observed after chitosan deposition and at this glutaraldehyde activation step as expected. We then introduced probe DNA solution which is terminated with amine group and assembled probe DNA on the chitosan film via glutaraldehyde. Figure 5-4 (d) shows that very weak fluorescence appears up to this assembly step due to the intrinsic fluorescence of the probe DNA. Next, we introduced aqueous solution of mismatch target DNA into the microchannel and Figure 5-4 (e) shows no significant fluorescence after this step, indicating that mismatch target DNA didn't react with probe DNA and also this result confirms that the mismatch target DNA didn't hybridize anywhere, as expected. Finally we introduced match target DNA

solution into the microchannel. Figure 5-4 (f) illustrates that match target DNA reacts with and becomes conjugated onto the probe DNA assembled on the activated chitosan scaffold. This result confirms that electrodeposited chitosan enables post-fabrication, *in situ* assembly of DNA in microfluidic channels through series of simple standard chemical reactions all in aqueous environment. Signal-guided sequential assembly of DNAs onto readily addressable sites is enabled in our microfluidic system. Importantly, probe DNA on the electrode retained its hybridization capacity throughout the assembly and hybridization procedures.



(a) Before chitosan deposition (b) chitosan solution introduction and electrodeposition of chitosan (c) Electrodeposited chitosan (d) Glutaraldehyde activation (e) Glutaraldehyde activated chitosan film (f) GFP reaction (g) GFP assembled on chitosan surface inside microchannel

Figure 5-1 Schematic process flow of GFP assembly on electrodeposited chitosan inside a microchannel

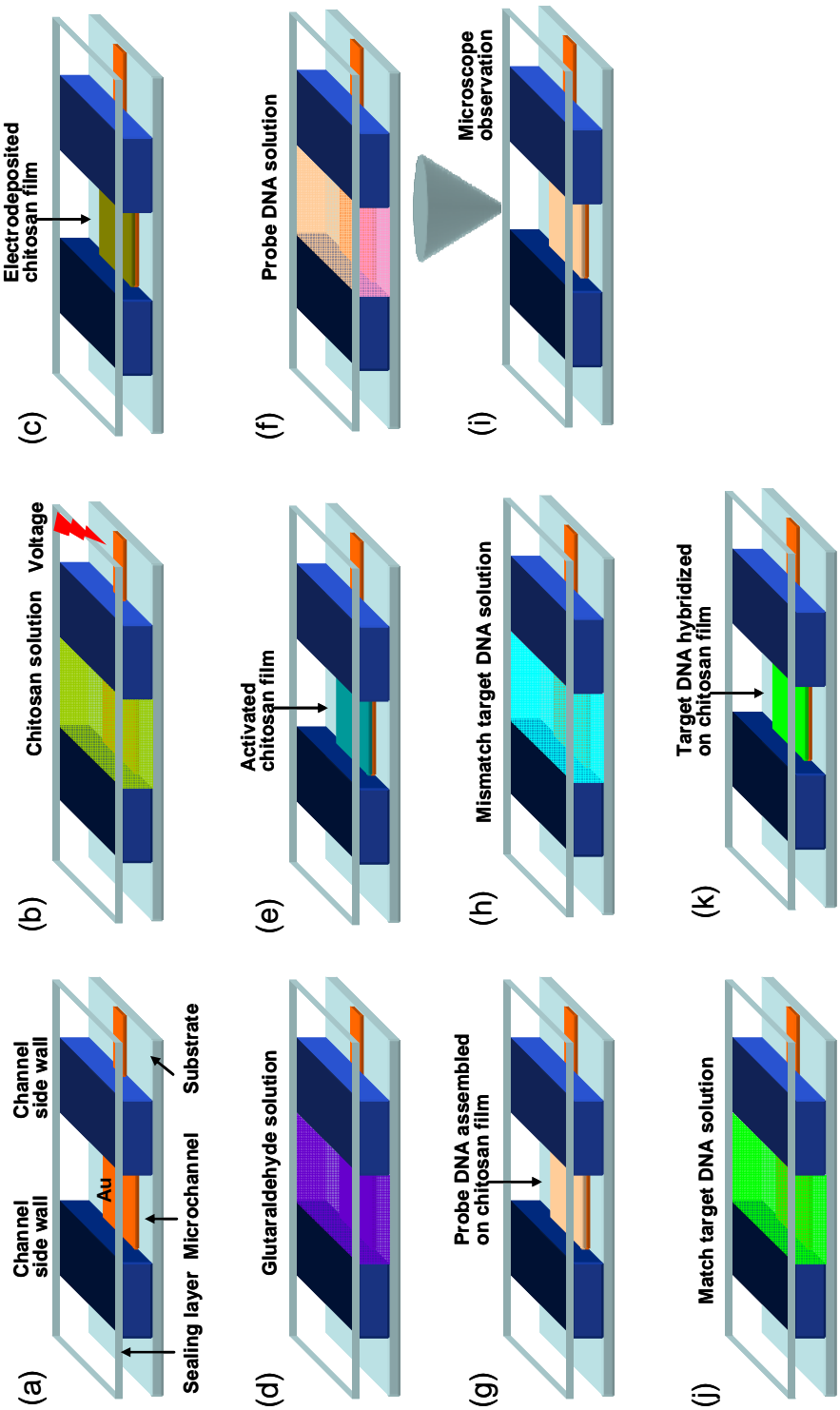


Figure 5-2 Schematic process flow of DNA hybridization on electrodeposited chitosan inside a microchannel

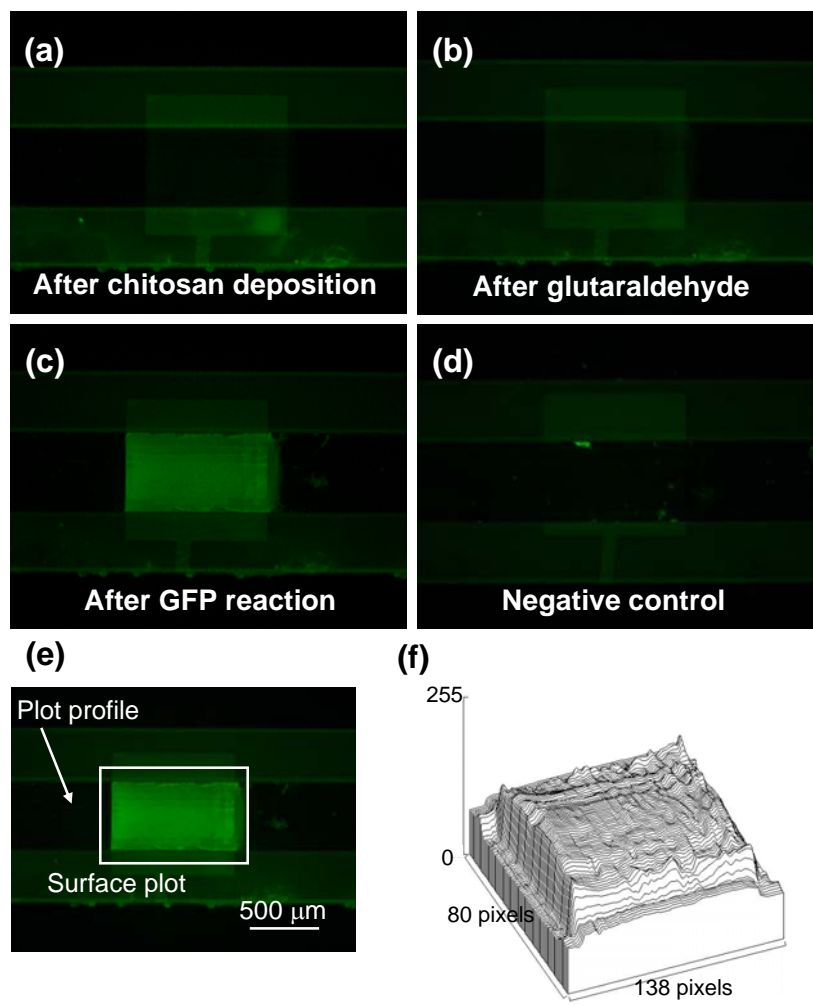


Figure 5-3 (a) Fluorescence image of the assembly site after chitosan deposition (b) After glutaraldehyde reaction (c) After GFP reaction (d) Negative control (no bias) (e) GFP conjugated chitosan film (f) Image J fluorescence surface plot

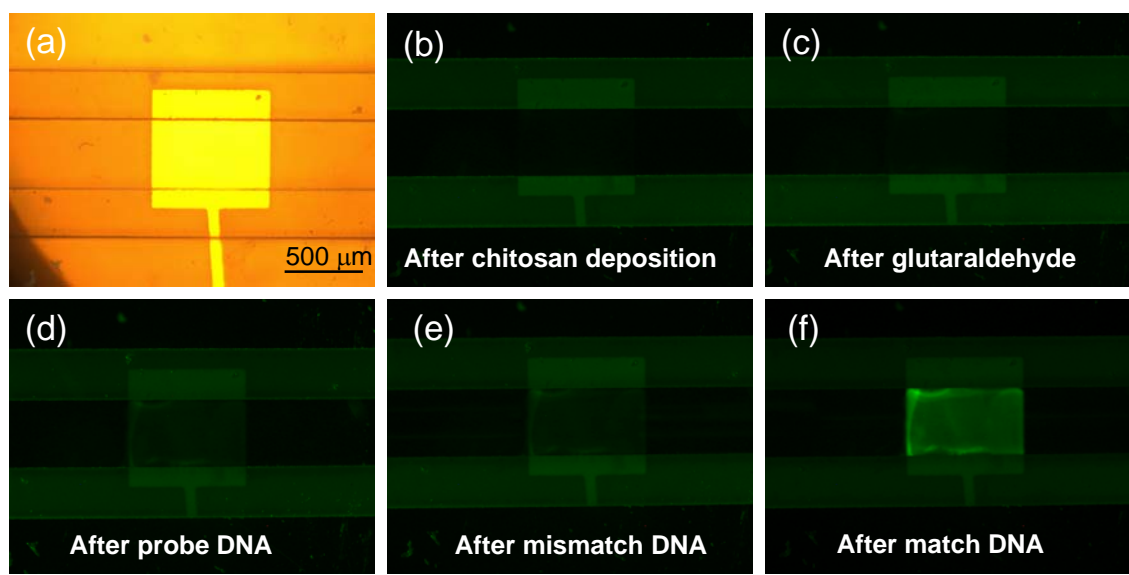


Figure 5-4 (a) Bright field image of assembly site (b) Fluorescence image of the assembly site after chitosan deposition (c) After glutaraldehyde reaction (d) After probe DNA reaction (e) Negative control (mismatch target DNA reaction) (f) After match target DNA hybridization

## **Chapter 6 Pfs-chitosan conjugate deposition and enzymatic reaction in completely packaged microfluidic devices**

### **6-1 Overview**

Bacterial intercellular communication provides a mechanism for the regulation of gene expression, resulting in coordinated population behavior via AI-2 (Autoinducer) signaling molecule. This phenomenon has been referred to as quorum sensing or cell-cell communication.<sup>74</sup> As a research plan, the idea of a microfluidic biomolecular factory is proposed and AI-2 signaling molecules are synthesized through multiple and sequential enzymatic reaction steps in the microfluidic channel. Figure 6-1 shows a schematic view of a microfluidic biomolecular factory arranged to synthesize the small molecule AI-2, an important cell signaling molecule. First Pfs (S-adenosylhomocysteine nucleosidase) and LuxS (S-ribosylhomocysteinase) enzymes conjugated with chitosan will be deposited on the separated assembly sites in the microchannel in sequence respectively. Then SAH (S-adenosylhomocysteine) precursor will be introduced and enzymatically converted to adenine and SRH (S-ribosylhomocysteine) by Pfs on the chitosan surface, following which the SRH will be similarly converted to AI-2 by the LuxS enzyme. To confirm the presence of AI-2, we put down a *Vibrio Harveyi* cell at the downstream of the LuxS-chitosan in the microchannel. It is known that a *Vibrio Harveyi* cell can detect AI-2 molecule and it leads to bioluminescence. In this thesis work we will attempt to demonstrate only the first step in the current microfluidic system. Pfs-chitosan conjugate is introduced into the microchannel and electrodeposited on the assembly site. SAH precursor is then flowed over the Pfs-chitosan and enzymatically converted to SRH and

Adenine. By-products adenine and SRH is collected and analyzed with HPLC (High Performance Liquid Chromatography) to determine the conversion rate of the enzymatic reaction. This experiment will demonstrate a portion of the metabolic pathway and an enzymatic biosynthesis reaction for biomolecular factory applications in microfluidic systems.

## **6-2 Pfs-chitosan conjugate electrodeposition and enzymatic reaction in microfluidic system**

Schematic drawing of enzymatic conversion of SAH precursor to SRH and adenine by assembled Pfs-chitosan inside the microchannel is shown in Figure 6-2. Solution of Pfs-chitosan conjugate was prepared for electrodeposition and enzymatic reaction experiment in the microfluidic system. We deposited Pfs-chitosan film inside the microchannel and SAH precursor was introduced over the Pfs-chitosan film and enzymatically converted to SRH and adenine product. First same cleaning steps were performed as described previously and PBS buffer was introduced into the microchannel for 30 min. BSA solution (2 g/l concentration) was introduced for 120 min, followed by PBS buffer rinsing for 30 min, prohibiting non specific binding of biomolecules on the microchannel. Pfs-chitosan conjugate solution was then introduced into the microchannel and deposited on the electrode ( $3A/m^2$ , 240 sec) in static fluidic condition.[Figure 6-2 (a) and (b)] PBS buffer was flowed over Pfs-chitosan film to rinse loosely attached excessive chitosan molecules for 30 min and then Tris buffer (trishydroxymethylaminomethane) was introduced to the microchannel for 10 min before SAH solution is introduced. The microchannel is in equilibrium condition for SAH

solution by introducing Tris buffer prior to SAH solution, since SAH solution is prepared in Tris buffer. Finally SAH precursor solution was then flowed over the Pfs-chitosan film in the microchannel for 60 min with 5  $\mu$ l/min flow rate and collected from the output of the microfluidic system every 5 min.[Figure 6-2 (c)] The collected samples were analyzed with HPLC and conversion rate from SAH to SRH and adenine was obtained.[Figure 6-2 (d)] *Ex situ* mechanical profilometer was also used to measure thickness of Pfs-chitosan film.

### **6-3 Result: Enzyme reaction in microfluidic system**

We demonstrate *in situ* enzymatic conversion of chemical substrate by electrodeposited enzyme–chitosan conjugate in the microfluidic channel. For this experiment, BSA solution was introduced into the microchannel to inhibit non specific binding on the surface of the microchannel. We then electrodeposited Pfs-chitosan conjugate film, followed by PBS buffer rinsing. Microchannel passed Tris buffer solution and SAH precursor was introduced into the microchannel. SAH precursor is enzymatically converted to adenine and SRH by Pfs on the chitosan surface. By-products adenine and SRH will be collected and analyzed with HPLC to determine the conversion rate of the enzymatic reaction. Figure 6-3 (a) shows HPLC analysis on the collected samples obtained from 2 different experiments which are experiment and negative control experiment. High intensity of adenine peak in the HPLC analysis on the collected samples shown on the left figure in Figure 6-3 (a) indicates that most of the SAH precursor was converted to adenine and SRH product by Pfs enzyme on the chitosan. In contrast, the right side figure of Figure 6-3 (a) shows a negative control channel, which

underwent the identical procedure as the previous channel except that the electrode was not negatively biased for Pfs-chitosan electrodeposition. The result indicates that most of SAH precursor was not converted to the product. This result reconfirms that the *in situ* enzymatic conversion was enabled by electrodeposited Pfs-chitosan in the microchannel. Small peak of adenine in the negative control experiment was observed and we speculate some dead volume in the microfluidic system provides Pfs-chitosan for the conversion from SAH to adenine and SRH. Finally Figure 6-3 (b) shows *ex situ* mechanical profilometry performed on the Pfs-chitosan structure inside the microchannel after disassembling the microfluidic system and the average thickness of the film was about 3  $\mu\text{m}$ . Combined these results demonstrate *in situ* signal-guided assembly of enzyme-chitosan and sequential enzymatic conversion of chemical precursor in the microfluidic system. This indicates the enzyme assembled with chitosan retains its biochemical reactivity throughout the assembly and enzymatic conversion procedure. This further could be exploited for rapid biosynthesis by implementing sequential multiple reaction steps in a microfluidic channel or for cell based sensor along with cell trapping device in a microfluidic channel.

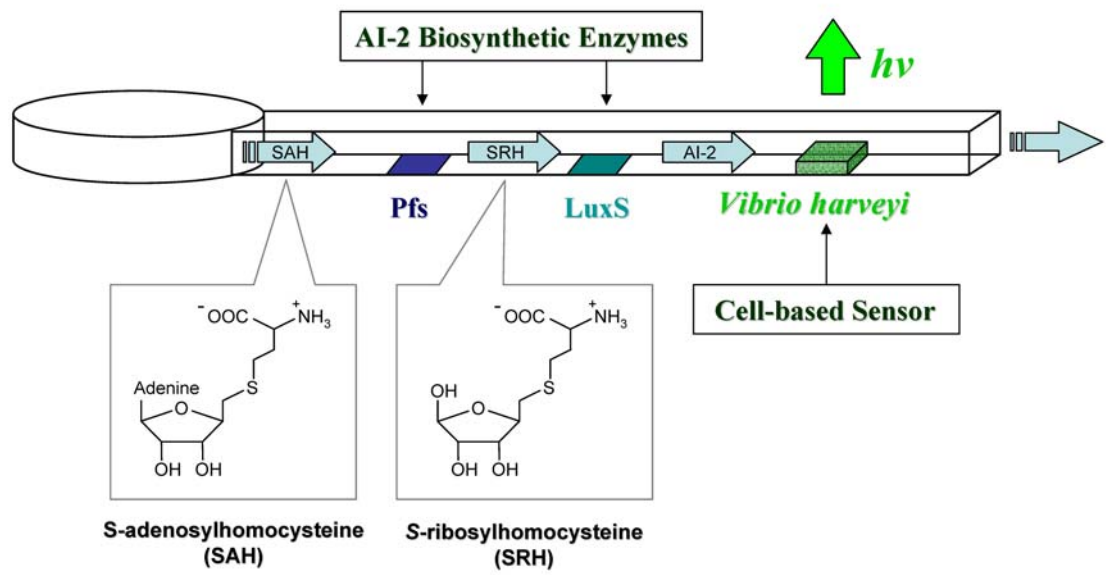


Figure 6-1 Schematic design of multiple enzymatic reaction in microfluidic channel for biomolecular factory application

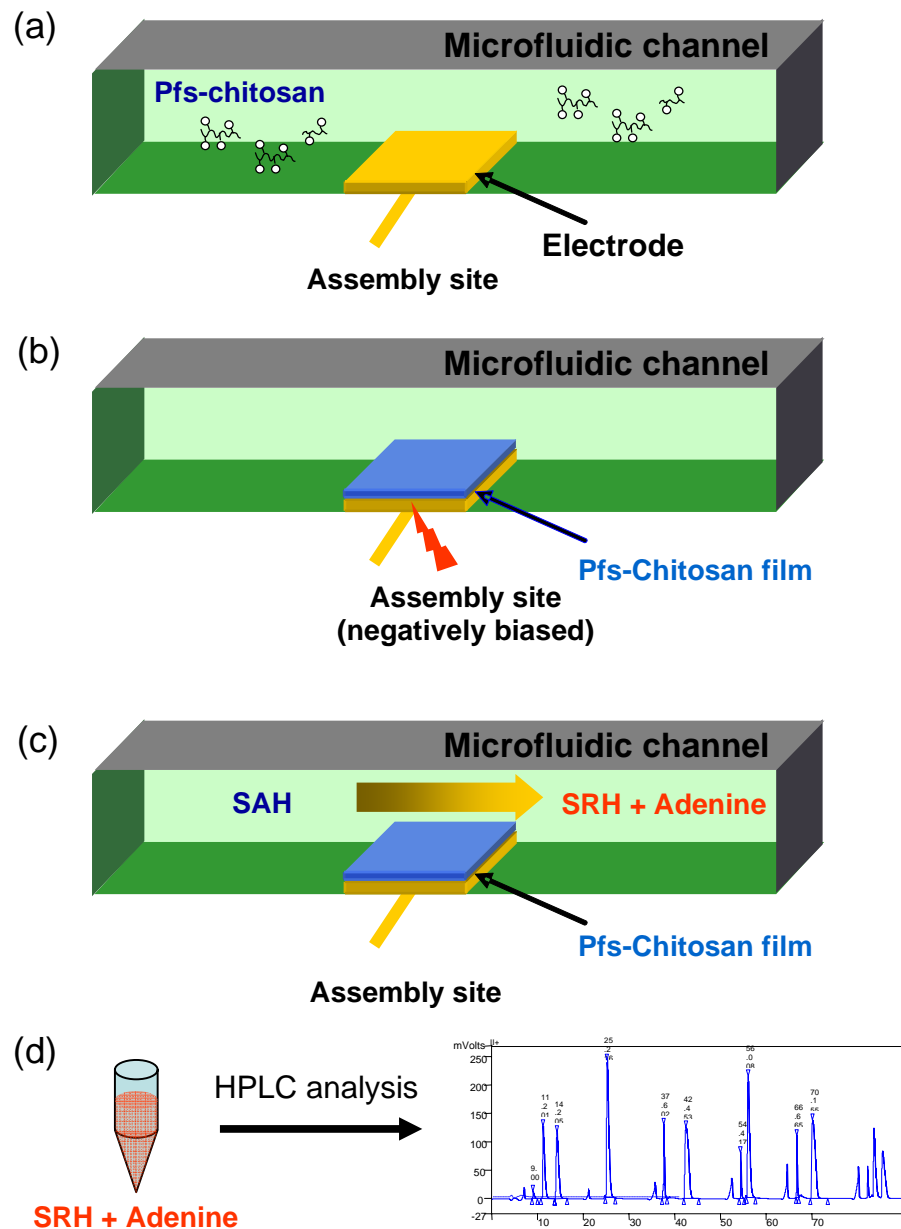


Figure 6-2 Schematic drawing of enzymatic conversion of SAH precursor to SRH and adenine by assembled Pfs-chitosan inside the microchannel (a) Pfs-chitosan conjugate introduction into microchannel (b) Electrodeposition of Pfs-chitosan (c) Enzymatic conversion of SAH precursor to SRH and adenine (d) HPLC analysis on the collected SRH and Adenine samples

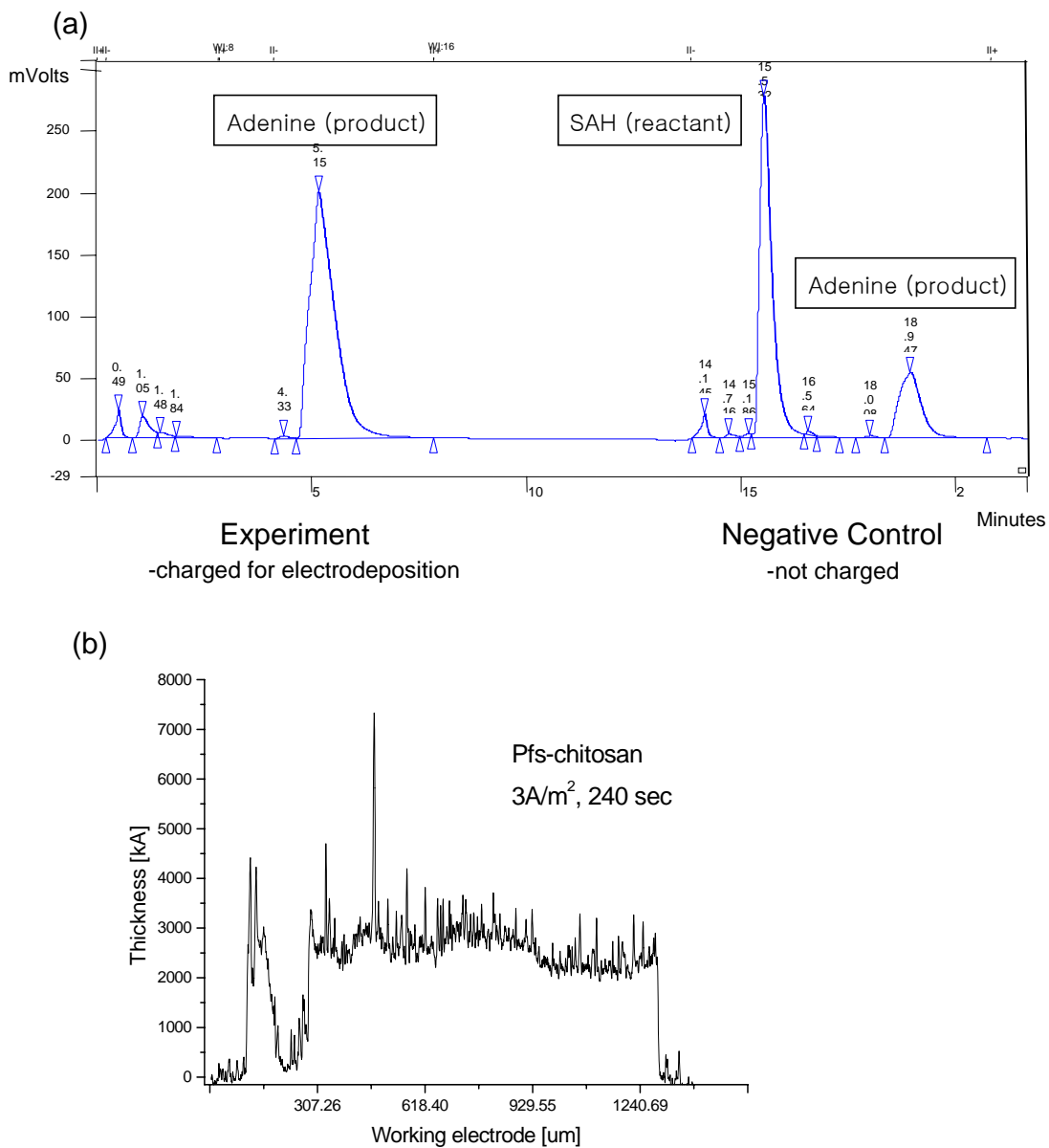


Figure 6-3 (a) HPLC analysis result of sample collected from microfluidic system; (left) Electrode was charged for chitosan deposition and SAH precursor introduced over electrodeposited chitosan film (right) Negative control experiment (electrode was not charged for chitosan deposition) (b) Mechanical profilometry on the electrodeposited Pfs-chitosan film inside the microchannel

## **Chapter 7 Conclusion**

This research represents post-fabrication biomolecule assembly at readily addressable sites inside the microfluidic channel after the device is completely packaged. Importantly, our assembly scheme exploits electrical signals to guide biomolecule assembly, which is distinct from conventional methods such as SAMs (Self Assembly Monolayers), microcontact printing, UV photo patterning and dip-pen nanolithography techniques that requires arduous chemical process, robotics and may hinder biofunctionalization at sites in three dimensional fluidic networks.

For this, we developed a microfluidic device with several unique features. In this work we have demonstrated a device and packaging approach well suited to our chitosan mediated biomolecule assembly technology. This technology is particularly suitable for bioMEMS systems employing spatially localized reaction sites for biomolecular conjugation and associated reaction processes. First, non-permanent packaging by flexible PDMS-spun on the top sealing plate and compression system bolts ensure consistent leak tight sealing as well as convenient *ex situ* analysis. Its micro-knife-edge compression sealing of SU8 microchannel sidewalls to a flexible PDMS gasket produces leak-free microfluidics, yet enables subsequent opening of the microfluidic system for component reuse and post-process examination of internal bio-structures. Second, the microfluidic system composed of all transparent materials allows simple *in situ* observation of the fluidic condition and biomolecule assembly processes by optical and/or fluorescence microscope. The approach employs polymeric materials – SU8, PDMS, and plastics – to achieve optical transparency as well as low cost, easy fabrication

and simplicity of the microfluidic device and package. Third, micropatterned gold electrodes at the bottom of the microfluidic channel provide sites for electrochemical activities inside the microchannel, allowing readily addressable and signal-guided biomolecule assembly. This approach enables post-fabrication, *in situ* biomolecule assembly in completely packaged microfluidic system. Finally, fluidic and electrical input/output ports provide fluid transport and electrical signal for the biomolecule assembly. These ports allow external fluidic/electrical system to directly control fluids and electrical signal inside the microchannel for bioreaction processes. The device and package design supports incorporation of microfluidic channels and networks, electrical signals at specific locations for programmable functionalization as well as diagnostics, and integration of optical waveguide structures as anticipated for lab on a chip application. Ultimately the strategy described here holds potential for multi-level microfluidic systems as well.<sup>75, 76</sup>

Harnessing this microfluidic device we then demonstrated spatially selective assembly of the device-biology interface chitosan by taking advantage of its pH-responsive property and chemically reactive properties. Indeed, our prior work has demonstrated covalent attachment of proteins, enzymes, DNA, RNA, and biopolymers to electrodeposited chitosan surfaces.<sup>55, 58</sup> Firstly, fluorescently labeled chitosan was deposited on the assembly site inside the microchannel, directly demonstrating *in situ* signal-guided biomolecule assembly on a specific electrode. We then demonstrated transport and covalent conjugation of marker molecule fluorescein and GFP onto the electrodeposited chitosan scaffold by taking advantage of its chemical reactivity. The results shown in Figure 4-5 and Figure 5-3 confirm the retained chemical reactivity of the

electrodeposited chitosan scaffold. Importantly, the electrodeposited chitosan was well retained throughout various transport and rinsing procedures, confirming its potential for biomolecule assembly scaffold for future applications. Further, the assembled GFP retained its fluorescence, suggesting that its structure remained intact through the assembly processes. Various biomolecules such as nucleic acid and enzyme assembly by mediating chitosan scaffold was also demonstrated inside the microchannel. Probe DNA is assembled on chitosan scaffold via glutaraldehyde crosslinking reagent and subsequent match DNA hybridization on the probe DNA confirms that electrodeposited chitosan enables post-fabrication, *in situ* assembly of DNA in microfluidic channels through series of simple standard chemical reactions all in aqueous environment. Importantly, probe DNA on the electrode retained its hybridization capacity throughout the assembly and hybridization procedures. We then demonstrated *in situ* signal-guided assembly of enzyme-chitosan and sequential enzymatic conversion of chemical precursor in the microfluidic system, indicating that the enzyme assembled with chitosan retains its biochemical reactivity throughout the assembly and enzymatic conversion procedure.

We have demonstrated this technology through the electrodeposition of chitosan, a biopolymer which is known to serve as a powerful platform for biomolecular conjugation and associated reactions. These results illustrate that biomolecules – represented by chitosan biopolymer – can be assembled at selected electrode sites in the microfluidic channels of a completed bioMEMS device, as proposed previously.<sup>55, 58</sup> Chitosan's unique properties – high amine site density and intermediate pKa – enables it to be electrodeposited in a spatially and temporally controllable manner, as well as to serve as scaffolds for multi site and multi step biomolecular conjugations and reactions for

bioMEMS applications.

We believe that our approach for biomolecule assembly in microfluidic devices offer several unique capabilities. First, the electric signal-guided nature of the chitosan assembly allows simple *in situ* assembly of biological molecules when and where it is needed, even long after the device is fully manufactured. BioMEMS devices utilizing biomolecules sensing capability has a short life time issue since biomolecules are assembled into the device during device manufacturing and may lose their reactivity during manufacturing or storage period. It is important that our approach employs post fabrication biomolecule assembly, allowing temporally programmable biomolecule assembly and is not limited by the device lifetime issue. This post fabrication biomolecule assembly technique may also allow biological components to be assembled into complex microfluidic networks (e.g. for high throughput drug screening) with greater ease than conventional assembly methods. Employed electrodeposition of chitosan and subsequent biomolecule assembly is performed in aqueous solution after a device is completely packaged, allowing biomolecule assembly on 2-D or 3-D structures. This advantage frees design of microfluidics aiming highly integrated device with complex fluidic network and multiplex functions for lab on a chip application. Second, biomolecules are assembled from the aqueous environment, thus preserving their biological activities through the assembly procedure. Since other conventional biomolecule assembly processes are performed in dried condition or leave assembled biomolecules in dried condition, biological activity may possibly be lost during device manufacturing or storage period. Electrodeposition of chitosan and subsequent biomolecule assembly is all performed in aqueous environment and reactivity of chitosan

and various biomolecules are retained during assembly processes, achieving more robust and reliable bioMEMS with post fabrication biomolecule assembly approach. Third, our approach is user friendly since the end-user, namely a biologist or a clinician, does not need complex robotic printing facilities or arduous chemical procedures to achieve selective biomolecule assembly. Finally, our technique may offer generic, flexible strategies for different target biomolecules (DNA, protein, enzyme, virus and cell) since a wide variety of conjugation schemes can be utilized for different biomolecules.<sup>58, 59, 68</sup> It also can be used to convert input reactants to desired products (e.g. small molecule catalysis); to simulate a metabolic pathway (e.g., for drug discovery and testing); to sense biochemical species; or to synthesize biomolecular products. Our robust leak tight and device integrated microfluidic system is requisite to achieve the purposes and various analysis techniques along with flexible microfluidic packaging scheme enable real time process monitoring and profound study on internal bio-structure inside microfluidics.

A number of advantages of microfluidics such as rapid bioreaction process, less human error, less contaminations, and small amount of reagents would still drive our bioMEMS research for lab on a chip applications. For long term goal, variety of sensing technique including optical waveguide, micro cantilever and mass spectrometer sensing will be integrated into the microfluidic system for improved controllability and observation on the active biofunctionalized site. Secondly, multiple bioreactions sites will be fabricated in a microfluidic channel along with micro valve and pumping actuators, enabling multiple bioreaction processes to be performed in more complex microfluidic network with enhanced fluid manipulation. Biomolecular factory, or microfluidic based microarray device would be fabricated and used for researches like

metabolic engineering, genomics or proteomics by employing complex microfluidic network and chitosan based biomolecule assembly scheme. Finally, microfluidics based cell sensing system will be developed. Researches on cell trapping and culturing have been started along with development of CMOS based transducer system and finally microfluidics integrate cell trapping device and transducers, providing powerful cell based sensor template for drug discovery, disease detection and fundamental metabolic engineering.

## **Chapter 8 Future work**

### **8-1 Multi steps of enzymatic reaction in microfluidic system**

We demonstrated the first step of the biomolecular factory which is *in situ* Pfs-chitosan assembly at readily addressable sites and SAH conversion to adenine and SRH in the microfluidic channels after complete fabrication and packaging of the microfluidic device.

HPLC results confirmed that the SAH precursor was successfully converted to adenine and SRH in the microchannel. It was the first step of our enzymatic biosynthesis process and Figure 8-1 (a) shows a schematic view of a microfluidic biomolecular factory arranged to synthesize the small molecule AI-2, an important cell signaling molecule. Bacteria communicate and coordinate behavior via this signaling molecule.

As a following work, the second step of the enzymatic biosynthesis process will be performed. A microfluidic device which employs multiple reaction sites for the Pfs-chitosan and Lux-chitosan assembly will be designed. It will allow the sequential electrodeposition of the Pfs-chitosan and Lux-chitosan in a single microfluidic channel, leading to the multi step enzymatic conversion from the SAH precursor to the AI-2 molecules.[Figure 8-1 (b)] The output of microfluidics will be collected and analyzed with HPLC to determine the conversion rate of the enzymatic reaction. This experiment will demonstrate the metabolic pathways and enzymatic biosynthesis reactions for biomolecular factory applications in microfluidic systems.

## **8-2 Integrated waveguide for real time optical detection of biocomponent in microfluidic system**

We demonstrated facile *in situ* biomolecule assembly in the microfluidic system after complete fabrication and packaging of the microfluidic device. The biomolecule assembly was mainly inspected by fluorescence microscope observation through the transparent microfluidic packaging system and *ex situ* analysis on the internal biostructure after opening the packaging system.

The *in situ* process sensing can be further developed by integrating an optical detection using planar waveguide on the active biofunctionalized site in the microfluidic system. This is the extension of Michael Powers' work into our microfluidic system and in his work, the design and fabrication of the waveguide and capacity testing were completed by using 635 nm laser on the fluorescently labeled chitosan deposited.[Figure 8-2 (a)]<sup>60</sup> The main future work remaining is to incorporate the output fibers into the package level.[Figure 8-2 (b)] The waveguides could easily be incorporated into the current microfluidic system by coupling optical fiber aligned to the waveguide in the microfluidic system since a single thick-film SU8 polymer layer has high refractive index. Therefore the SU8 waveguide can be fabricated along with microfluidic channels simultaneously on the same substrate. Chitosan-mediated biomolecule assembly can occurs at the side wall of the microchannel and intersect the optical path. Integrated optical detection of signal guided biomolecule assembled in microfluidic system will be a significant advance toward future applications in complex biomolecular or biosensing analyses as anticipated for future lab on a chip.

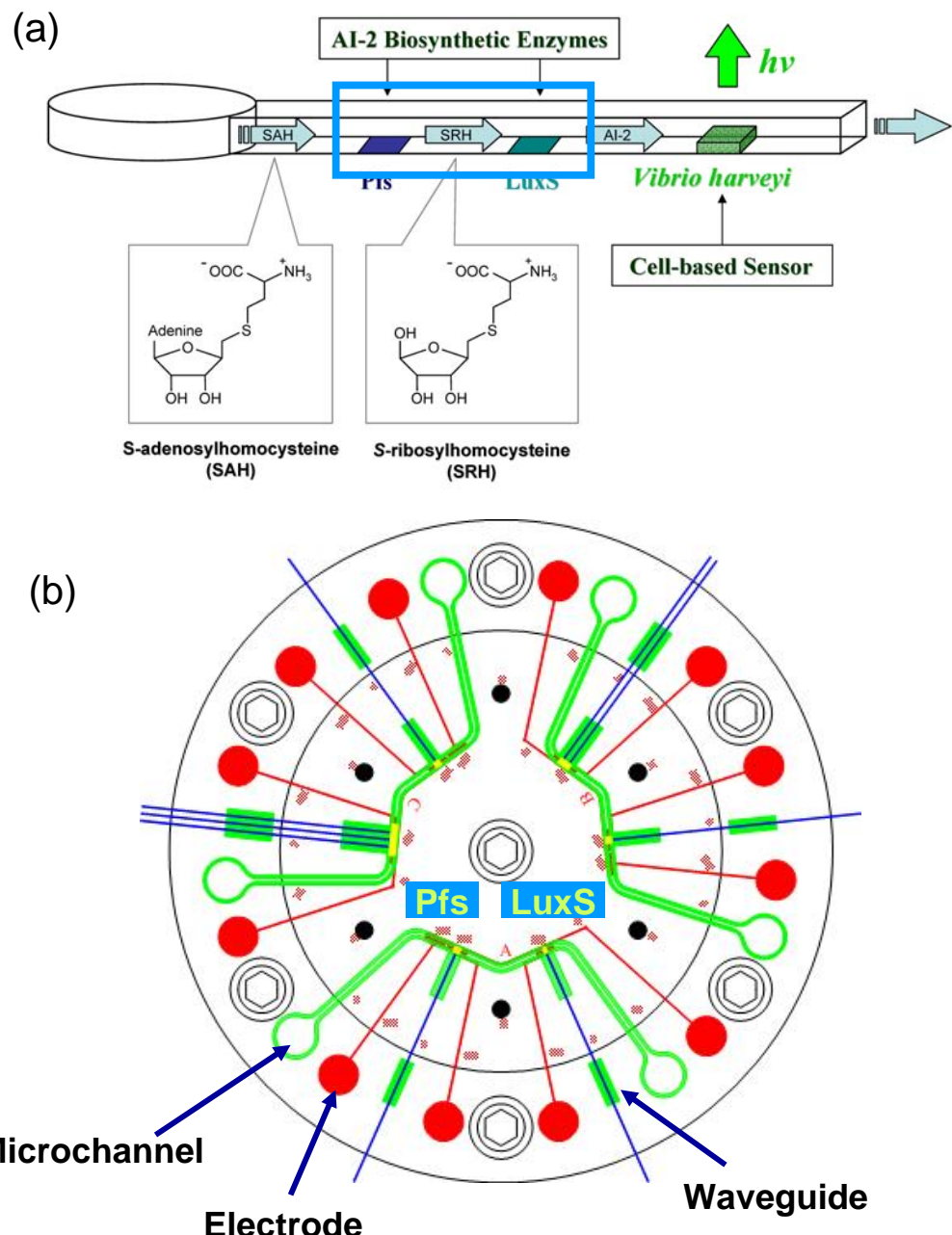


Figure 8-1 (a) Schematic design of multiple enzymatic reaction in microfluidic channel for biomolecular factory application (b) Microfluidic system design for biomolecular factory

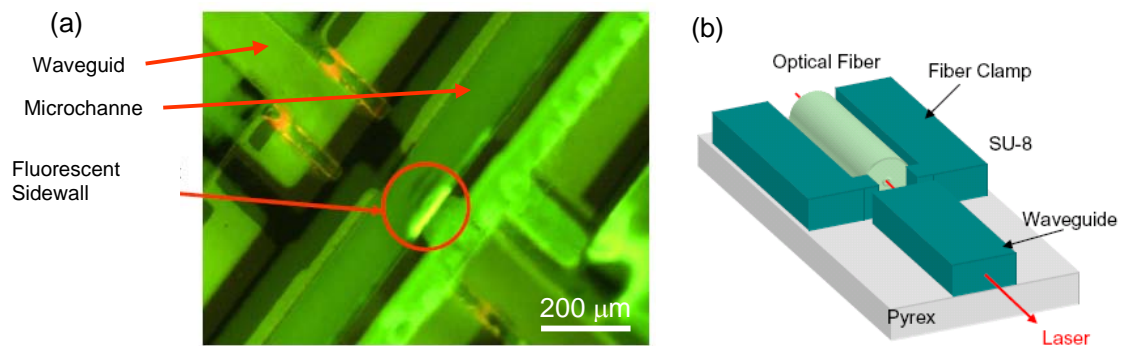


Figure 8-2 (a) Fluorescent micrograph with a green fluorescein dye chitosan conjugate indicating successful sidewall deposition (b) 3-D image of fiber alignment structure.

## BIBLIOGRAPHY

- <sup>1</sup> K. J. Gabriel, *Proceedings of the Ieee*, 1998, **86**, 1534.
- <sup>2</sup> K. W. Markus and K. J. Gabriel, *Computer*, 1999, **32**, 25.
- <sup>3</sup> W. P. Eaton and J. H. Smith, *Smart Materials & Structures*, 1997, **6**, 530.
- <sup>4</sup> L. P. Wang, R. A. Wolf, Y. Wang, K. K. Deng, L. C. Zou, R. J. Davis, and S. Trolier-McKinstry, *Journal of Microelectromechanical Systems*, 2003, **12**, 433.
- <sup>5</sup> P. F. Van Kessel, L. J. Hornbeck, R. E. Meier, and M. R. Douglass, *Proceedings of the Ieee*, 1998, **86**, 1687.
- <sup>6</sup> D. L. Polla, A. G. Erdman, W. P. Robbins, D. T. Markus, J. Diaz-Diaz, R. Rizq, Y. Nam, H. T. Brickner, A. Wang, and P. Krulevitch, *Annual Review of Biomedical Engineering*, 2000, **2**, 551.
- <sup>7</sup> D. Peichel, D. Marcus, R. N. Rizq, A. G. Erdman, W. P. Robbins, and D. L. Polla, *Journal of Microelectromechanical Systems*, 2002, **11**, 154.
- <sup>8</sup> E. Renard, *Minimally Invasive Therapy & Allied Technologies*, 2004, **13**, 78.
- <sup>9</sup> G. H. W. Sanders and A. Manz, *Trac-Trends in Analytical Chemistry*, 2000, **19**, 364.
- <sup>10</sup> M. J. Heller, *Annual Review of Biomedical Engineering*, 2002, **4**, 129.
- <sup>11</sup> M. Krishnan, V. Namasivayam, R. S. Lin, R. Pal, and M. A. Burns, *Current Opinion in Biotechnology*, 2001, **12**, 92.
- <sup>12</sup> J. Wang, M. P. Chatrathi, B. M. Tian, and R. Polksy, *Analytical Chemistry*, 2000, **72**, 2514.
- <sup>13</sup> R. Raiteri, G. Nelles, H. J. Butt, W. Knoll, and P. Skladal, *Sensors and Actuators B-Chemical*, 1999, **61**, 213.
- <sup>14</sup> A. M. Moulin, S. J. O'Shea, and M. E. Welland, *Ultramicroscopy*, 2000, **82**, 23.
- <sup>15</sup> R. D. Oleschuk and D. J. Harrison, *Trac-Trends in Analytical Chemistry*, 2000, **19**, 379.
- <sup>16</sup> M. A. Burns, *Science*, 2002, **296**, 1818.
- <sup>17</sup> D. R. Reyes, D. Iossifidis, P. A. Auroux, and A. Manz, *Analytical Chemistry*, 2002, **74**, 2623.
- <sup>18</sup> P. A. Auroux, D. Iossifidis, D. R. Reyes, and A. Manz, *Analytical Chemistry*, 2002, **74**, 2637.

- <sup>19</sup> A. P. Blanchard, R. J. Kaiser, and L. E. Hood, *Biosensors & Bioelectronics*, 1996, **11**, 687.
- <sup>20</sup> T. Wink, S. J. vanZuilen, A. Bult, and W. P. vanBennekom, *Analyst*, 1997, **122**, R43.
- <sup>21</sup> T. M. Herne and M. J. Tarlov, *Journal of the American Chemical Society*, 1997, **119**, 8916.
- <sup>22</sup> L. A. Chrisey, G. U. Lee, and C. E. OFerrall, *Nucleic Acids Research*, 1996, **24**, 3031.
- <sup>23</sup> S. A. Lange, V. Benes, D. P. Kern, J. K. H. Horber, and A. Bernard, *Analytical Chemistry*, 2004, **76**, 1641.
- <sup>24</sup> Y. N. Xia and G. M. Whitesides, *Annual Review of Materials Science*, 1998, **28**, 153.
- <sup>25</sup> M. J. Tarlov, D. R. F. Burgess, and G. Gillen, *Journal of the American Chemical Society*, 1993, **115**, 5305.
- <sup>26</sup> R. D. Piner, J. Zhu, F. Xu, S. H. Hong, and C. A. Mirkin, *Science*, 1999, **283**, 661.
- <sup>27</sup> K. B. Lee, S. J. Park, C. A. Mirkin, J. C. Smith, and M. Mrksich, *Science*, 2002, **295**, 1702.
- <sup>28</sup> J. Kameoka, H. G. Craighead, H. W. Zhang, and J. Henion, *Analytical Chemistry*, 2001, **73**, 1935.
- <sup>29</sup> A. Hatch, A. E. Kamholz, K. R. Hawkins, M. S. Munson, E. A. Schilling, B. H. Weigl, and P. Yager, *Nature Biotechnology*, 2001, **19**, 461.
- <sup>30</sup> A. G. Hadd, D. E. Raymond, J. W. Halliwell, S. C. Jacobson, and J. M. Ramsey, *Analytical Chemistry*, 1997, **69**, 3407.
- <sup>31</sup> L. L. Sohn, O. A. Saleh, G. R. Facer, A. J. Beavis, R. S. Allan, and D. A. Notterman, *Biophysical Journal*, 2001, **80**, 144A.
- <sup>32</sup> P. Belgrader, M. Okuzumi, F. Pourahmadi, D. A. Borkholder, and M. A. Northrup, *Biosensors & Bioelectronics*, 2000, **14**, 849.
- <sup>33</sup> B. A. Buchholz, E. A. S. Doherty, M. N. Albarghouthi, F. M. Bogdan, J. M. Zahn, and A. E. Barron, *Abstracts of Papers of the American Chemical Society*, 2001, **222**, U93.
- <sup>34</sup> I. K. Glasgow, H. C. Zeringue, D. J. Beebe, S. J. Choi, J. T. Lyman, N. G. Chan, and M. B. Wheeler, *Ieee Transactions on Biomedical Engineering*, 2001, **48**, 570.
- <sup>35</sup> J. Yang, Y. Huang, X. B. Wang, F. F. Becker, and P. R. C. Gascoyne, *Analytical Chemistry*, 1999, **71**, 911.
- <sup>36</sup> L. E. Locascio, C. E. Perso, and C. S. Lee, *Journal of Chromatography A*, 1999, **857**, 275.

- <sup>37</sup> M. A. Roberts, J. S. Rossier, P. Bercier, and H. Girault, *Analytical Chemistry*, 1997, **69**, 2035.
- <sup>38</sup> D. C. Duffy, J. C. McDonald, O. J. A. Schueller, and G. M. Whitesides, *Analytical Chemistry*, 1998, **70**, 4974.
- <sup>39</sup> M. A. Schmidt, *Proceedings of the Ieee*, 1998, **86**, 1575.
- <sup>40</sup> E. R. Perez, *Adhesives Age*, 1994, **37**, 25.
- <sup>41</sup> H. Becker and L. E. Locascio, *Talanta*, 2002, **56**, 267.
- <sup>42</sup> D. M. Leatzow, J. M. Dodson, J. P. Golden, and F. S. Ligler, *Biosensors & Bioelectronics*, 2002, **17**, 105.
- <sup>43</sup> D. J. Beebe, G. A. Mensing, and G. M. Walker, *Annual Review of Biomedical Engineering*, 2002, **4**, 261.
- <sup>44</sup> A. Hiratsuka, H. Muguruma, K. H. Lee, and I. Karube, *Biosensors & Bioelectronics*, 2004, **19**, 1667.
- <sup>45</sup> C. H. Ahn, J. W. Choi, G. Beaucage, J. H. Nevin, J. B. Lee, A. Puntambekar, and J. Y. Lee, *Proceedings of the Ieee*, 2004, **92**, 154.
- <sup>46</sup> D. Kim and M. L. Shuler, *Proceedings of the SPIE - The International Society for Optical Engineering*, 2004, **5321**, 309.
- <sup>47</sup> T. Fujii, *Microelectronic Engineering*, 2002, **61-2**, 907.
- <sup>48</sup> J. W. Choi, K. W. Oh, J. H. Thomas, W. R. Heineman, H. B. Halsall, J. H. Nevin, A. J. Helmicki, H. T. Henderson, and C. H. Ahn, *Lab on a Chip*, 2002, **2**, 27.
- <sup>49</sup> D. J. Harrison, K. Fluri, K. Seiler, Z. H. Fan, C. S. Effenhauser, and A. Manz, *Science*, 1993, **261**, 895.
- <sup>50</sup> L. Bousse and W. Parce, *Ieee Engineering in Medicine and Biology Magazine*, 1994, **13**, 396.
- <sup>51</sup> G. J. M. Bruin, *Electrophoresis*, 2000, **21**, 3931.
- <sup>52</sup> J. Liu, C. Hansen, and S. R. Quake, *Analytical Chemistry*, 2003, **75**, 4718.
- <sup>53</sup> S. P. A. Fodor, J. L. Read, M. C. Pirrung, L. Stryer, A. T. Lu, and D. Solas, *Science*, 1991, **251**, 767.
- <sup>54</sup> C. D. Bain, E. B. Troughton, Y. T. Tao, J. Evall, G. M. Whitesides, and R. G. Nuzzo, *Journal of the American Chemical Society*, 1989, **111**, 321.
- <sup>55</sup> H. M. Yi, L. Q. Wu, R. Ghodssi, G. W. Rubloff, G. F. Payne, and W. E. Bentley, *Analytical Chemistry*, 2004, **76**, 365.
- <sup>56</sup> L. Q. Wu, A. P. Gadre, H. M. Yi, M. J. Kastantin, G. W. Rubloff, W. E. Bentley, G. F. Payne, and R. Ghodssi, *Langmuir*, 2002, **18**, 8620.

- 57 L. Q. Wu, H. M. Yi, S. Li, G. W. Rubloff, W. E. Bentley, R. Ghodssi, and G. F. Payne, *Langmuir*, 2003, **19**, 519.
- 58 H. M. Yi, L. Q. Wu, R. Ghodssi, G. W. Rubloff, G. F. Payne, and W. E. Bentley, *Langmuir*, 2005, **21**, 2104.
- 59 H. M. Yi, L. Q. Wu, W. E. Bentley, R. Ghodssi, G. W. Rubloff, J. N. Culver, and G. F. Payne, *Biomacromolecules*, 2005, **6**, 2881.
- 60 M. A. Powers, S. T. Koev, A. Schleunitz, H. M. Yi, V. Hodzic, W. E. Bentley, G. F. Payne, G. W. Rubloff, and R. Ghodssi, *Lab on a Chip*, 2005, **5**, 583.
- 61 W. Tan and T. A. Desai, *Biomedical Microdevices*, 2003, **5**, 235.
- 62 Z. L. Zhang, C. Crozatier, M. Le Berre, and Y. Chen, *Microelectronic Engineering*, 2005, **78-79**, 556.
- 63 R. Fernandes, L. Q. Wu, T. H. Chen, H. M. Yi, G. W. Rubloff, R. Ghodssi, W. E. Bentley, and G. F. Payne, *Langmuir*, 2003, **19**, 4058.
- 64 S. D. Senturia, '*Microsystem Design*', Kluwer Academic Publishers, 2002.
- 65 J. J. Park, T. Valentine, M. Anderle, R. Ghodssi, and G. W. Rubloff, IVC-16/ICSS-12/NANO-8/AIV-17, Venice, Italy, 2004.
- 66 R. Fernandes, H. M. Yi, L. Q. Wu, G. W. Rubloff, R. Ghodssi, W. E. Bentley, and G. F. Payne, *Langmuir*, 2004, **20**, 906.
- 67 R. Canteri, C. Pederzolli, L. Lunelli, L. Pasquardini, M. Vinante, S. Forti, G. Speranza, L. Vanzetti, J. Park, G. Rubloff, and M. Anderle, AVS 51st International Symposium & Exhibition, Anaheim, CA, 2004.
- 68 H. M. Yi, S. Nisar, S. Y. Lee, M. A. Powers, W. E. Bentley, G. F. Payne, R. Ghodssi, G. W. Rubloff, M. T. Harris, and J. N. Culver, *Nano Letters*, 2005, **5**, 1931.
- 69 J. Carlier, S. Arscott, V. Thomy, J. C. Fourrier, F. Caron, J. C. Camart, C. Druon, and P. Tabourier, *Journal of Micromechanics and Microengineering*, 2004, **14**, 619.
- 70 H. Lorenz, M. Despont, N. Fahrni, N. LaBianca, P. Renaud, and P. Vettiger, *Journal of Micromechanics and Microengineering*, 1997, **7**, 121.
- 71 X. G. Li, T. Abe, Y. X. Liu, and M. Esashi, *Journal of Microelectromechanical Systems*, 2002, **11**, 625.
- 72 K. R. Williams, K. Gupta, and M. Wasilik, *Journal of Microelectromechanical Systems*, 2003, **12**, 761.
- 73 B. Keiper, H. Exner, U. Loschner, and T. Kuntze, *Journal of Laser Applications*, 2000, **12**, 189.
- 74 A. L. Beeston and M. G. Surette, *Journal of Bacteriology*, 2002, **184**, 3450.

<sup>75</sup> M. A. Unger, H. P. Chou, T. Thorsen, A. Scherer, and S. R. Quake, *Science*, 2000, **288**, 113.

<sup>76</sup> T. Thorsen, S. J. Maerkli, and S. R. Quake, *Science*, 2002, **298**, 580.